Optimal Resilient Operation of Multi-Carrier Energy Systems in Electricity Markets Considering Distributed Energy Resource Aggregators

Hamid Zakernezhad [1], Mehrdad Setayesh Nazar[1], Miadreza Shafie-khah[2], and João P. S. Catalão[3,*]

[1] *Shahid Beheshti University, Tehran, Iran*

[2] *School of Technology and Innovations, University of Vaasa, 65200 Vaasa, Finland*

[3] *Faculty of Engineering of the University of Porto and INESC TEC, 4200-465 Porto, Portugal*

[*] *catalao@fe.up.pt*

Abstract

This paper presents a novel iterative three-level optimization framework for the optimal resilient operational scheduling of active multi-carrier energy generation and distribution systems. The main contribution of this paper is that the proposed framework simulates the day-ahead and real-time pre-event preventive and post-event corrective actions for external shocks and explores the effectiveness of risk-averse operational strategies on the system's costs. The solution methodology is another contribution of this paper that finds the optimal scheduling of distributed energy resources and switching of electrical switches and district heating and cooling control valves. At the first stage, the optimal day-ahead scheduling of distributed energy resources and the initial value of the risk control parameter are determined using robust optimization. At the second stage, the optimal real-time market scheduling of distributed energy resources is performed. Finally, at the third stage, different extreme shock scenarios are considered, the effectiveness of corrective actions are investigated, and the value of risk control parameter is modified. The proposed method was successfully applied to the modified 123-bus test system and 600 scenarios of external shocks were considered. The proposed process successfully reduced the expected cost of the 123-bus system by about 74.59% for the worst-case external shock. Further, the algorithm reduced the aggregated expected values of operational and interruption costs by about 57.73% for all of the 600 cases of the considered external shocks.

Keywords: Combined cooling, heating and power; Multi-energy carriers; Demand response program; Resilient operation.

Nomenclature

Abbreviation

ACH	Absorption Chillers.
EGDS	Energy Generation and Distribution Systems.
ARIMA	Autoregressive Integrated Moving Average.
CCH	Compression Chiller.
CCHP	Combined Cool, Heat and Power.
CSS	Cool Storage System.
CERTS	Consortium for Electric Reliability Technology Solutions.
CHP	Combined Heating and Power.
DER	Distributed Energy Resource.
DG	Distributed Generation.
DLC	Direct Load Control.
DRP	Demand Response Program.
ESS	Electrical Storage System.
MUs	Monetary Units.
MMUs	Million MUs.
PHEV	Plug-in Hybrid Electric Vehicle.
PHEVA	Plug-in Hybrid Electric Vehicle Aggregator.
PV	Photovoltaic.
OROS	Optimal Resilient Operational Scheduling.
WT	Wind Turbine.
TES	Thermal Energy Storage.

Parameters

C^{CHP}	Operational costs of CHP unit (MUs).
C^{ESS}	Operational costs of electricity storage (MUs).
C^{TES}	Operational costs of thermal storage (MUs).
C^{CSS}	Operational costs of cool storage (MUs).
C^{DG}	Operational costs of distributed generation (MUs).
C^{Boiler}	Operational costs of boiler (MUs).
C^{ACH}	Operational costs of absorption chiller (MUs).
C^{CCH}	Operational costs of compression chiller (MUs).
C^{DLC}	Cost of direct load control (MUs).
C^{PHEVAs}	Cost of PHEVAs commitment (MUs).
C^{TOU}	Cost of time-of-use program (MUs).
COP_{ACH}	Coefficient of performance of absorption chiller.

COP_{CCH}	Coefficient of performance of compression chiller.
Cap^{CSS}	Capacity of cooling storage (kW).
$F^{\max}$	Maximum flow of electrical line (kW).
$H_{Critical}^{Load}$	Critical heating load (kW).
$H_{Controllable}^{Load}$	Controllable heating load (kW).
$IC_{Electrical}$	Interruption cost electrical load (MU/kWh).
$IC_{Heating}$	Interruption cost heating load (MU/kWh).
$IC_{Cooling}$	Interruption cost cooling load (MU/kWh).
$NCEL$	Number of critical electric load.
$NCHL$	Number of critical heating load.
$NCCL$	Number of critical cooling load.
$NPHEVAS$	Total number of PHEVAs contribution scenarios.
$NDAMS$	Total number of day-ahead market price scenarios.
$NRTMS$	Total number of real-ahead market price scenarios.
$NTOUS$	Total number time-of-use scenarios.
$NEXSS$	Total number of external shock scenarios.
$Nzone$	Number of EGDS zones.
P^{DRP}	Demand response program electric power generation/reduction (kW).
P^{Load}	Electric power of electrical load (kW).
P^{PVA}	Electric power generated by photovoltaic array (kW).
P^{ESS}	Electric power delivered by electricity storage (kW).
$P_{Critical}^{Load}$	Critical electrical load (kW).
$P_{Controllable}^{Load}$	Controllable electrical load (kW).
$P_{Deferrable}^{Load}$	Deferrable electrical load (kW).
P^{WT}	Electric power generated by WT (kW).
$R_{Critical}^{Load}$	Critical cooling load (kW).
$R_{Controllable}^{Load}$	Controllable cooling load (kW).
$prob$	Probability.
ϖ_{PHEVA}^{Charge}	Charge limitation ratio.
$\varpi_{PHEVA}^{Discharge}$	Discharge limitation ratio.
ρ_{Active}^{DA}	Active power purchasing price that is purchased from the day-ahead upward market (MUs/kWh).
ρ_{Active}^{RT}	Active power purchasing price that is purchased from the real-ahead upward market (MUs/kWh).

$\rho_{rective}^{DA}$ Reactive power purchasing price that is purchased from the day-ahead upward market (MUs/kVARh).

$\rho_{rective}^{RT}$ Reactive power purchasing price that is purchased from the real-ahead upward market (MUs/kVARh).

λ^{active} Active power price sold to the upward market (MUs/kW).

$\lambda^{reactive}$ Reactive power price sold to the upward market (MUs/kVAR).

$\lambda^{cooling}$ Cooling power price sold to the cooling loads (MUs/kW).

$\lambda^{heating}$ Heating power price sold to the heating loads (MUs/kW).

ϑ Maximum discharge coefficient of cooling storage.

T Total operational scheduling horizon of first stage problem (Hour).

τ Total operational scheduling horizon of second stage problem (Hour).

τ' Total operational scheduling horizon of third stage problem (Hour).

Γ Robustness level parameter.

Variables

ΔC_{NSZ} Change in operating cost of neighbour suppling zone (MU).

$ENPHEVA$ State of charge of PHEVA parking lot.

$ENSC$ Energy not supplied cost (MUs/kWh).

H Heating power (kW).

H^{Loss} Loss of heating power (kW).

H^{Flow} Transferred heating power through district heating pipeline (kW).

ΔH^{DLC} Heating power withdrawal changed for direct load control program (kW).

$NESAZone$ Number of external shock affected zone.

$NSUPZone$ Number of supplying zones.

P Electrical active power (kW).

$P^{Transaction}$ Active power transacted with the upward market (kW).

ΔP^{TOU} Electric power injection/withdrawal changed for time-of-use program (kW).

ΔP^{DLC} Electric power withdrawal changed for direct load control program (kW).

PCH^{PHEVA} PHEVA active power charge (kW).

$PDCH^{PHEVA}$ PHEVA active power discharge (kW).

Q Electrical reactive power (kVAR).

R	Cooling power (kW).
R^{Loss}	Cooling power loss (kW).
R^{Flow}	Transferred cooling power through district cooling pipeline (kW).
RC^{CSS}	Cool storage charging power (kW).
RDC^{CSS}	Cooling power discharge of cooling storage (kW).
ΔR^{DLC}	Cooling power withdrawal changed for direct load control program (kW).
x	State variable.
X^{CSS}	Binary variable of cooling storage discharge; equal to 1 if cooling storage is discharged.
y	Control variable.
Y^{CSS}	Binary variable of cooling storage charge; equal to 1 if cooling storage is charged.
z	Topology variable.
V	Voltage of EGDS bus (kV).
δ	Voltage angle of EGDS bus (rad).
φ	Binary decision variable of device/program operation/utilization (equal to 1 if device operates).
ψ^{Switch}	Binary decision variable of switching device (equal to 1 if device operates).
ψ^{DHV}	Binary decision variable of district heating control valve (equal to 1 if device operates).
ψ^{DCV}	Binary decision variable of district cooling control valve (equal to 1 if device operates).
$\Xi(x,u,z)$	Equality constraints.
$\Omega(x,u,z)$	Inequality constraints.
Θ	Dual variable of inner-step optimization of the first objective function.
u'	Dual variable of inner-step optimization of the first objective function.
γ^{-R}	Expected price of real-ahead market price.
P^{R}	Active power transaction with the real-ahead upward market.
ξ	Deviation from the expected value of real-ahead market price.
v	Auxiliary variable.

1. Introduction

The multi-carrier Energy Generation and Distribution System (EGDS) concept is widely accepted due to integrating energy systems, increasing efficiency of energy conversion, reducing the transmission loss, and decreasing the emission of pollutants. An EGDS can utilize different Distributed Energy Resources (DERs) to supply its electrical, heating, and cooling loads through its energy transmission systems. However, the EGDS must tolerate the external shocks that may be imposed on its distributed systems, continue to deliver multi-carrier energy to its customers, and recover to a new stable condition of operation [1]. The external shocks may be natural disasters or anthropogenic hazards in a way that their exact location, intensity, and duration may be unknown before the occurrence.

The resilience operation of EGDS is a crucial issue in the operation of infrastructures from both the economic and social stability points of view. However, there are a few types of research in the resilient operational paradigms of an active multi-carrier energy system in the recent literature. As shown in Table 1, the literature can be categorized into the following two categories.

The first category of papers explored the resilient operational scheduling of the electric distribution system. Ref. [2] proposed a two-stage optimization algorithm to quantify the resiliency of an electric distribution system and determine the optimal topology of the distribution system. The proposed algorithm utilized a resiliency index to reconfigure the system using the analytical hierarchical process. Ref. [3] introduced a metaheuristic optimization algorithm to coordinate the DERs of the electrical distribution system. The optimal formation of microgrids was determined and the effectiveness of the method was assessed for the 33-bus IEEE test system. The proposed two-layer optimization algorithm optimized the topology and operational scheduling of the system in the first and second layers, respectively. Ref. [4] proposed a three-step procedure to enhance the resilience of an electric distribution system. At the first step, the resilience and hardening preparation process was considered. In the second step, the switching actions were performed to form a multi-microgrids system and increase the system resiliency. In the third stage, the final steps of service restoration were carried out. Ref. [5] proposed an algorithm for supplying critical loads in the islanded operation of the system. The procedure minimized the aggregated critical load shedding and maximized the served non-critical loads. The adjustable loads and Plug-in Hybrid Electric Vehicles (PHEVs) were considered in the model and a mixed-integer non-linear programming optimization algorithm was utilized. Ref. [6] quantified the resiliency level of an electric distribution system by using an approximate path finding method for supplying microgrids after the external shock occurrence. The proposed method utilized dependency-based indices to form the microgrids. The proposed algorithms were assessed by using two different test systems. Ref. [7] proposed a model for the interaction of electric and natural gas systems in contingent conditions. The framework utilized a two-stage robust optimization procedure to assess the performance of the electric system in the contingent conditions. Ref. [8] proposed an algorithm to determine the vulnerable components of the system. The optimization method performed the preventive actions, minimized the operational cost of the multiple microgrids, and enhanced the resiliency of the system. Ref. [9] introduced an algorithm to split the electric system into multi-microgrids in contingent conditions. The multi-objective function was solved using the Pareto optimality method and the algorithm was assessed for the 33-bus and 69-bus test systems. Ref. [10] proposed a model to minimize load curtailments in the contingent condition of the system. The algorithm considered the normal and resilient operation conditions and a robust optimization procedure was performed to consider the operational uncertainties. Ref. [11] proposed a self-healing strategy for a distribution system in the normal and self-healing conditions. The algorithm minimized the operational costs in the normal operational mode. Further, the system was sectionalized into networked microgrids to supply the critical loads in the self-healing mode. The uncertainties of energy resources and loads were considered and the case study was

carried out for the 123-bus test system. Ref. [12] proposed an optimal coordinated energy management strategy for multi-microgrid systems using the multi-objective optimization process. Ref. [13] introduced a two-stage optimization algorithm to determine the optimal topology of the distribution system after contingency using graph theory. In the first step, the optimal partitioning procedure was utilized and in the second stage, the optimal load shedding values were determined. Ref. [14] proposed a microgrid formation model that considered energy loss and voltage constraints. A mixed-integer linear programming model was utilized to consider the nonlinearity of the system and an iteration based linear approximation was considered to solve the model. Ref. [15] presented a resiliency-based modelling framework for restoration strategies of electric distribution systems. A resiliency measure was utilized to determine the resiliency level of the system and consider the response-time of the components. The model was assessed for a test system with 180-component system constituted of lines, laterals, and transformers.

Refs. [2-15] proposed the optimal DERs scheduling and electric system switching for the pre-event and/or post-event conditions. However, the optimal resilient scheduling of multi-carrier EGDS and switching of district heating and cooling control valves were not considered in these papers. These references did not integrate the model of heating and cooling loads, chillers, multiple distributed energy resource aggregators, and switching of district heating and cooling control valves in their models. Hence, the present paper simultaneously considers the described models and the switching of control valves, pre-event preventive actions, and on-event corrective actions.

The second category of papers considered the optimal operational scheduling of electric distribution system that transacted energy with the non-utility DERs and the upward electricity market. Ref. [16] proposed a two-level optimization framework to minimize the system costs and the peak loads. The uncertainty of intermittent electricity generation was also modelled. Ref. [17] introduced a two-stage robust optimization model for the multi-microgrids to minimize the operating cost of the system. The worst-case scenarios of intermittent electricity generation were considered. Ref. [18] minimized the operating costs and maximized the reliability of the system using a meta-heuristic algorithm. Ref. [19] introduced a two-stage algorithm to schedule the PHEVs and modify the load profile. The responsive loads were utilized to compensate the uncertainties of intermittent DERs. Ref. [20] optimized the day-ahead operational scheduling of an industrial Combined Heat and Power (CHP) system. Ref. [21] proposed an algorithm to minimize the operational and reliability costs using bat stochastic optimization model. The uncertainties of the intermittent electricity generations and the PHEVs were modelled. Ref. [22] proposed a robust optimization method for scheduling of the CHP-based system using information gap method. Ref. [23] presented a two-stage mixed-integer linear programming stochastic optimization algorithm to minimize the operating costs of the system. A scenario-based method was used to model the uncertainties of the DERs and loads. Ref. [24] introduced a framework for optimizing energy exchanges between electrical energy storages and PHEVs and the model considered the uncertainties of electric vehicle loads. Further, the optimal bidding strategy of charging stations was presented. Ref. [25] introduced a two-level optimization process to schedule resources of a distribution system that transacted electricity with the downward multi-microgrids.

Ref. [26] presented an integrated framework for optimal operation of DERs, demand response programs, and PHEVs for an electrical distribution system. Ref. [27] proposed a two-stage scheduling procedure for an electrical distribution system. In the first stage, the DERs capacity was dispatched and in the second stage, the deviations from the forecasts were minimized.

However, the optimal resilient scheduling of multi-carrier EGDS was not considered in these papers [16-27]. Refs. [16-27] do not consider the security constraints of the system, switching of tie-switches and control valves, the heating and cooling loads of system, and real-time market. Based on the above literature survey, a framework that considers the described models, pre-event preventive actions and post-event corrective actions optimization is less frequent in the previous papers.

Hence, this paper proposes an integrated model that considers multiple distributed energy resource aggregators consisting of Plug-in Hybrid Electric Vehicle Aggregators (PHEVAs) and demand response aggregators. In the proposed model, the EGDS can utilize fossil-fuelled Distributed Generations (DGs), CHP units, photovoltaic systems, wind turbines, electrical energy storages, thermal energy storages, boilers, absorption chillers, compression chillers, cool storage systems, and district heating and cooling network to supply its loads. The EGDS can sell its surplus electricity to the upward wholesale market, participate in day-ahead and real-time electricity market, and optimally dispatch its DERs to enhance its system resiliency. The proposed model considers the security constraints system, the commitment process of system's heating and cooling loads, real-time market, and switches and control valves.

Table 1 shows a comprehensive comparison of the proposed model with the other papers. The proposed framework considers the optimal scheduling of the EGDS electrical, heating and cooling energy resources, electric switches, and heating and cooling control valves.

The main contributions of this paper can be summarized as:

- The proposed three-stage algorithm considers optimal preventive/corrective scheduling of distributed electrical, heating, and cooling energy resources.
- Several sources of uncertainty are considered: 1) The upward day-ahead electricity market price; 2) The day-ahead electrical, heating, and cooling loads; 3) The day-ahead charge and discharge of PHEVAs; 4) The day-ahead intermittent electricity generation; 5) The day-ahead electricity consumption; 6) The upward real-time electricity market price; 7) The parameters of imposed shocks.
- The proposed framework determines the optimal risk-averse control parameter for the extreme shocks and explores the effectiveness of the corrective actions on the external shock impacts.
- The model considers the impacts of DERs commitment on the post-event corrective actions to reduce the consequences of external shocks.

Table 1: Comparison of the proposed model with other papers.

References		2	3	4	5	6	7	8	9	10	11	12	13	14	15	16	17	18	19	20	21	22	23	24	25	26	27	Proposed Approach
Method	MILP	×	×	×	×	×	×	✓	×	✓	×	×	×	×	×	✓	×	×	×	✓	×	×	✓	×	×	×	✓	×
	MINLP	×	×	×	✓	×	×	×	×	×	✓	×	×	✓	×	×	×	×	×	×	×	✓	×	×	×	×	×	×
	Heuristic	✓	✓	✓	×	✓	✓	×	✓	×	×	✓	✓	×	✓	×	✓	✓	✓	×	✓	×	×	×	✓	✓	×	✓
Model	Deterministic	✓	✓	✓	✓	✓	✓	✓	✓	✓	×	×	✓	✓	×	×	×	✓	×	✓	×	×	×	×	×	×	×	×
	Stochastic	×	×	×	×	×	×	×	×	×	✓	✓	×	×	×	✓	✓	×	✓	×	✓	✓	✓	✓	✓	✓	✓	✓
Objective Function	Revenue	×	×	×	×	×	×	×	×	×	×	×	×	×	×	×	×	×	×	×	×	✓	×	×	×	✓	×	✓
	Gen. Cost	✓	✓	✓	×	×	✓	✓	✓	✓	✓	×	✓	×	×	✓	×	✓	✓	×	×	✓	✓	×	✓	✓	×	✓
	Storage Cost	×	✓	×	✓	×	×	×	×	×	×	×	×	×	×	×	✓	✓	×	×	×	×	✓	✓	✓	×	✓	✓
	Secu. Costs	✓	×	✓	×	✓	✓	✓	✓	✓	✓	✓	✓	✓	✓	×	×	×	✓	×	✓	×	×	×	×	×	×	✓
	PHEV cost	×	×	×	×	×	×	×	×	×	×	✓	×	×	×	×	✓	×	✓	×	✓	×	×	✓	×	×	×	✓
	DRP costs	×	✓	×	×	×	×	×	×	×	×	×	×	×	×	×	×	✓	✓	✓	×	×	✓	×	✓	✓	×	✓
	WT	×	✓	×	✓	×	×	×	×	×	×	×	×	×	×	×	×	✓	✓	×	✓	×	✓	×	×	×	×	✓
	PV	×	✓	×	×	×	×	×	×	×	×	✓	×	×	×	×	✓	✓	✓	×	✓	×	✓	×	×	×	✓	✓
CHP Nonlinearity		×	×	×	×	×	×	×	×	×	×	×	×	×	×	×	×	×	×	✓	×	✓	✓	×	×	×	×	✓
Optim. levels	Pre-event	✓	✓	✓	×	×	✓	✓	✓	✓	✓	✓	×	✓	✓	×	×	×	×	×	×	×	×	×	×	×	×	✓
	Post-event	✓	✓	✓	✓	✓	✓	✓	×	✓	✓	✓	✓	×	×	×	×	×	×	×	×	×	×	×	×	×	×	✓
Day-ahead Market		×	×	✓	×	×	×	×	×	×	×	×	×	×	×	×	✓	✓	✓	✓	✓	✓	✓	✓	✓	✓	✓	✓
Real-time market		×	×	×	×	×	×	×	×	×	×	×	×	×	×	×	✓	×	×	×	×	×	×	×	×	×	×	✓
Multiple energy carriers dispatch		×	×	×	×	×	✓	✓	×	×	×	×	×	×	×	×	×	×	×	×	×	×	×	×	×	×	×	✓
Uncertainty Model	PHEV	×	×	×	×	×	×	×	×	×	×	✓	×	×	×	×	✓	×	✓	×	✓	×	×	✓	×	×	×	✓
	DRP	×	×	×	×	×	×	×	×	×	×	×	×	×	×	×	×	×	×	×	×	×	✓	×	×	✓	✓	✓
	Day-ahead Market	×	×	×	×	×	×	×	×	×	×	×	×	×	×	×	×	×	×	✓	×	×	×	×	×	×	✓	✓
	Real-time market	×	×	×	×	×	×	×	×	×	×	×	×	×	×	×	×	×	×	×	×	×	×	×	×	×	✓	✓
	External Shock	×	×	×	×	×	×	×	×	×	×	×	×	×	×	×	×	×	×	×	×	×	×	×	×	×	×	✓
	Loads	×	×	×	×	×	×	×	×	×	×	×	×	×	×	×	×	×	✓	✓	×	×	✓	✓	×	×	✓	✓
	Interm .Elec.G.	×	×	×	×	×	×	×	×	×	×	✓	×	×	×	×	✓	×	✓	✓	✓	×	×	×	×	✓	✓	✓
Storage System	EES	×	✓	×	×	×	×	×	×	×	×	✓	×	×	×	✓	✓	✓	×	✓	✓	×	×	✓	✓	✓	✓	✓
	TES	×	×	×	×	×	×	×	×	×	×	×	×	×	×	×	×	×	×	×	×	×	✓	×	×	×	×	✓
	CSS	×	×	×	×	×	×	×	×	×	×	×	×	×	×	×	×	×	×	×	×	×	×	×	×	×	×	✓
AC model		×	✓	×	✓	×	×	×	✓	×	×	✓	✓	✓	×	✓	×	✓	×	×	×	×	×	✓	✓	✓	×	✓
Reconf. of heating and cooling system		×	×	×	×	×	×	×	×	×	×	×	×	×	×	×	×	×	×	×	×	×	×	×	×	×	×	✓

2. Problem Modelling and Formulation

The EGDS transacts energy with the upward electricity market in the day-ahead and real-time markets, and supplies its electrical, heating and cooling loads. Further, the EGDS can transact electricity with the PHEVAs and demand response aggregators. The Optimal Resilient Operational Scheduling (OROS) of EGDS consists of the optimal commitment of the system resources in the day-ahead and real-time markets considering the stochastic behaviour of optimization data, dynamic interdependency of electrical, heating and cooling systems, characteristics of devices, and economic analysis.

As shown in Fig. 1, the EGDS utilizes DGs, Combined Cool, Heat and Power (CCHP) units, photovoltaic systems, wind turbines, thermal energy storages, boilers, absorption chillers, compression chillers, and cool storage systems. The described OROS problem has different sources of uncertainties that are considered in the next subsection.

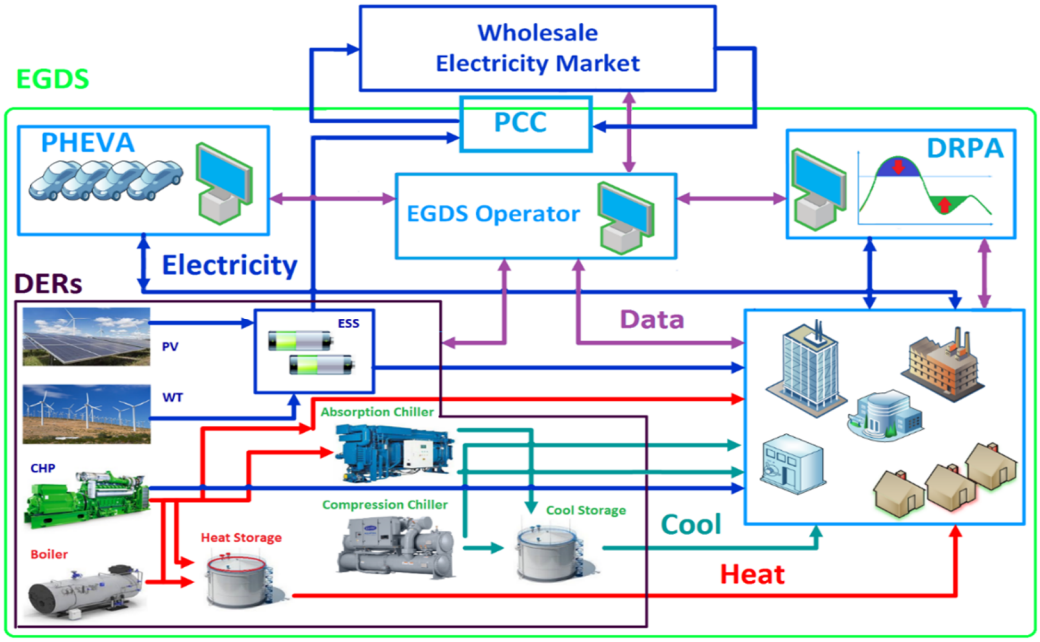

Fig. 1. The EGDS energy resources and transactions.

2.1. Demand response program aggregator modelling

The EGDS electrical loads consist of critical, deferrable, and controllable loads [28]. The deferrable loads can be shifted to off-peak hours using a time-of-use price procedure. Further, direct load control can be utilized to commit the controllable loads. The load shifting and direct load control procedures are presented by the demand response aggregators. Thus, the electrical loads can be written as [28]:

$$P^{Load} = P^{Load}_{Critical} + P^{Load}_{Deferrable} + P^{Load}_{Controllable} \tag{1}$$

$$\Delta P^{TOU} = P^{Load}_{Deferrable} \tag{2}$$

$$\sum_{t=1}^{Period} \Delta P^{TOU} = 0 \tag{3}$$

$$\Delta P_{Min}^{TOU} \le \Delta P^{TOU} \le \Delta P_{Max}^{TOU} \tag{4}$$

$$\Delta P_{Min}^{DLC} \le \Delta P^{DLC} \le \Delta P_{Max}^{DLC} \ , \Delta P_{Max}^{DLC} = P_{Controllable}^{Load} \tag{5}$$

$$P^{DRP} = \Delta P^{DLC} + \Delta P^{TOU} \tag{6}$$

Hence, the direct load control and time-of-use loads are considered as dispatchable control variables for the EGDS. However, the time-of-use loads have a stochastic behaviour that should be considered in the OROS modelling.

2.2. PHEV aggregator modelling

The PHEVAs have parking lots in the EGDS zones. To model the behaviour of PHEVs, these assumptions are considered [29]:

1. All PHEVs have the same batteries.
2. PHEVAs are independent of each other.

The historical data is used to compute the probability density function [29]. The PHEVAs energy balance and the energy limit constraints can be formulated as (7) and (8), respectively:

$$EPHEVA(t) = EPHEVA(t-1) + \varpi_{PHEVA}^{Charge}.PCH^{PHEVA}(t).\Delta t - \frac{1}{\varpi_{PHEVA}^{Discharge}}.PDCH^{PHEVA}.\Delta t \tag{7}$$

$$ENPHEVA^{min} \le ENPHEVA \le ENPHEVA^{max} \tag{8}$$

$$0 \le PCH^{PHEVA} \le PCH^{PHEVA,Max} \tag{9}$$

$$0 \le PDCH^{PHEVA} \le PDCH^{PHEVA,Max} \tag{10}$$

The EGDS dispatches the PHEVAs as dispatchable resources. The constraints of PHEVAs should be considered in the optimization process.

2.3. Uncertainty modelling

A seven-level uncertainty modelling can be performed for the proposed problem. At the first and second levels of uncertainty modelling, the EGDS estimates the upward day-ahead electricity market prices and multi-carrier energy loads, respectively. At the third and fourth levels of uncertainty modelling, the EGDS estimates the PHEVAs charge/discharge and the intermittent electricity generations, respectively. At the fifth level, the day-ahead time-of-use electricity consumption scenarios are generated. At the sixth and seventh levels of uncertainty modelling, the market prices for real-time horizon electricity and external shocks parameters are estimated. The external shocks are categorized into extreme, expected, and routine shocks. Their characteristics are shown in Table 2.

Table 2. The external shocks categories.

External Shock Category	Shocks
Extreme	Triple electric line outage
	Triple DG outage
	Triple CHP outage
	More than 20% of electricity generation facilities outage
	More than 20% of heating energy generation facilities outage
	More than 20% of cooling energy generation facilities outage
	Combination of above shocks
Expected	Double electric line outage
	Double DG outage
	Double CHP outage
	Single line and double DG/CHP outage
	Combination of above shocks
Routine	Single line and DG/CHP outage
	Double line outage

The maximum anticipated external shock is categorized as an extreme external shock. It is assumed that the EGDS system is segmented into different zones and each zone is adequately designed to tolerate the expected external shocks, routine external shocks, and the N-1 system contingencies [9]. Thus, the capacity of DERs of each zone is adequate to supply the electrical, heating and cooling loads. Hence, the cool storage system, thermal energy storage, and electrical energy storage of each zone can be dispatched in preventive actions, and they can be committed for the optimal corrective actions. In addition, each EGDS zone is equipped with switching devices, and heating and cooling on/off control valves. These switching facilities and control valves can be used for transacting electricity, heating, and cooling energy carriers in contingent conditions.

2.4. The proposed OROS procedure

A three-stage optimization process is proposed for the OROS procedure. As shown in Fig. 2, the EGDS determines the optimal commitment of DERs for the day-ahead horizon and utilizes the preventive actions to mitigate the impact of the estimated external and internal shocks. Then, the EGDS updates its databases in the real-time operation process and utilizes the second stage of OROS. The third stage of the proposed OROS is continuously carried out to explore the effectiveness of the probable corrective actions and determine the impact of shocks in an on-event corrective actions procedure.

If the corrective action simulation results cannot reduce the impact of the shocks, then the risk control parameter is modified and the preventive dispatch of the system is optimized. Further, the corrective action simulations are performed again and the procedure is repeated. The details of the three-stage optimization procedure are presented in the next subsections.

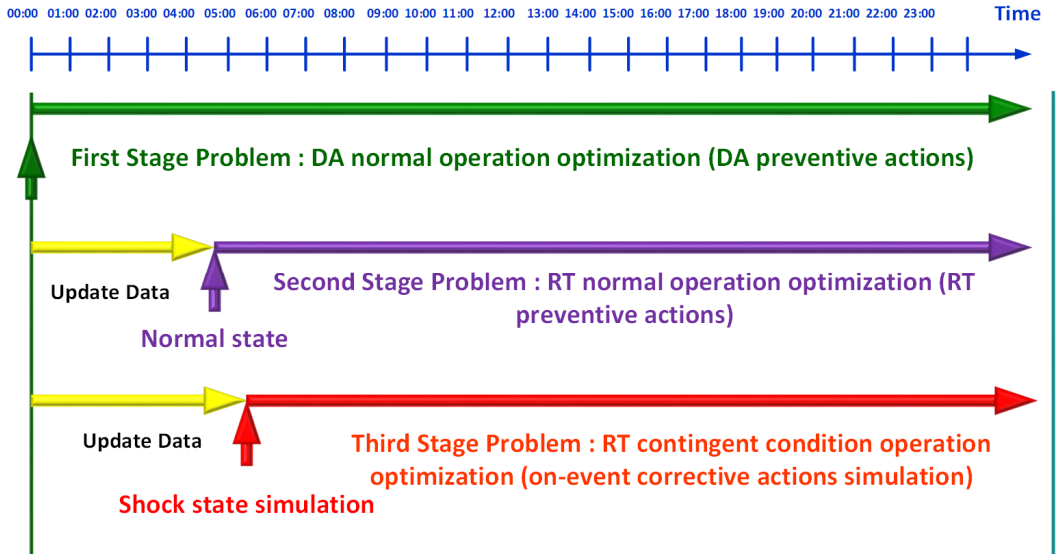

Fig. 2. The OROS process in the day-ahead and real-time horizon.

2.5. The first stage problem

As shown in Fig. 2, a three-level optimization algorithm is proposed. The first-stage problem considers the preventive actions in the day-ahead horizon for the probable extreme external shocks. The control variables of the EGDS are the commitment of CHPs, electrical energy storages, thermal energy storages, cool storage systems, DGs, boilers, absorption chillers, compression chillers, and direct load controls.

Further, the electricity transactions with the upward electricity market, PHEVAs, and time-of-use are the control variables that are modelled as stochastic processes. The EGDS can reconfigure its electrical system to perform a preventive action against external shock. Thus, the day-ahead preventive actions scheduling problem can be formulated as a multi-objective optimization process. The first stage objective function determines the optimal DERs commitment schedule and minimizes the expected operational costs and energy not supplied costs for the day-ahead horizon. In addition, the objective function minimizes the voltage deviations of the electrical system for the expected extreme external shock conditions. The first stage problem can be formulated as (11):

$$
\begin{aligned}
Min\ \mathbf{Z} = \sum^{T}\sum^{Nzone} \Bigg(& C^{CHP}.\varphi^{CHP} + C^{ESS}.\varphi^{ESS} + C^{TES}.\varphi^{TES} + C^{CSS}.\varphi^{CSS} + C^{DG}.\varphi^{DG} \\
& + C^{Boiler}.\varphi^{Boiler} + C^{ACH}.\varphi^{ACH} + C^{CCH}.\varphi^{CCH} + C^{DLC}.\varphi^{DLC} \\
& + \sum^{NPHEVAS} prob.C^{PHEVAs}.\varphi^{PHEVAs} \pm \sum^{NDAMS} prob.\rho^{DA}_{Active}.P^{Transaction}.\varphi^{DA}_{Active} \\
& \pm \sum^{NDAMS} prob.\rho^{DA}_{reactive}.Q^{Transaction}.\varphi^{DA}_{reactive} \pm \sum^{NRTMS} prob.\rho^{RT}_{Active}.P^{Transaction}.\varphi^{DA}_{Active} \\
& \pm \sum^{NRTMS} prob.\rho^{RT}_{reactive}.Q^{Transaction}.\varphi^{DA}_{reactive} + \sum^{TOUS} prob.C^{TOU}.\varphi^{TOU} \\
& + \sum^{NEXSS} prob.ENSC - revenue \Bigg)
\end{aligned}
\tag{11}
$$

$$
s.t.: \quad \Xi_1(x,u,z) = 0
$$

$$
\Omega_1(x,u,z) \geq 0
$$

Eq. (11) consists of the following parameters: 1) CHPs, electrical energy storages, thermal energy storages, cool storage systems, DGs, boilers, absorption chillers, compression chillers, and direct load control costs; 2) the expected cost of energy purchased from PHEVAs; 3) the expected active power cost/benefit that is transacted with the upward electricity market; 4) the expected reactive power cost/benefit that is transacted with the upward electricity market; 5) the expected costs of time-of-use loads; 6) the ENSCs of external shocks; 7) and the revenue of electrical, heating and cooling energy sold to customers.

The revenue of EGDS can be written as (12):

$$revenue = \left(\sum \lambda^{active}.P^{Load} + \sum \lambda^{reactive}.Q^{Load} + \sum \lambda^{heating}.H^{heating} + \sum \eta^{cooling}.R^{cooling} \right) \quad (12)$$

The revenue consists of the electrical active and reactive power, heating power and cooling power that are sold to the customers. It is assumed that the electricity transaction with the upward electricity market is performed within a predefined power factor.

The wind turbines and photovoltaic facilities are equipped with the electrical energy storages and their electricity generation can be dispatched by the EGDS. Thus, their electricity generation costs should be considered in the electrical energy storage costs. The constraints of the objective functions of the first stage problem are categorized as the following groups.

A. Electrical power balance

The electrical power balance constraint can be written as (13) [28]:

$$-\sum P^{Load} \pm \sum P^{ESS} \pm \sum P^{PHEVA} + \sum P^{CHP} - \sum P^{ACH} - \sum P^{CCH} \pm \sum P^{DRP} \quad (13)$$
$$-P^{Loss} \mp P^{Transaction} = 0$$

The same formulation can be written for reactive power balance constraints.

B. Heating and cooling power balance

The heating and cooling power balance constraints can be written as (14) and (15), respectively [28]:

$$-\sum H^{Load} + \sum H^{Boiler} - \sum H^{ACH} + \sum H^{CHP} \pm \sum H^{TES} + H^{Loss} + \sum H^{Flow} = 0 \quad (14)$$

$$-\sum R^{Load} + \sum R^{CCH} + \sum R^{ACH} - R^{Loss} \pm \sum R^{CSS} + \sum R^{Flow} = 0 \quad (15)$$

$$P^{CCH} = \frac{R^{CCH}}{COP_{CCH}} \quad (16)$$

$$H^{ACH} = \frac{R^{ACH}}{COP_{ACH}} \quad (17)$$

$$\frac{R^{ACH}}{COP_{ACH}} \le Q^{CHP} \quad (18)$$

C. Thermal energy storage, cool storage system and electrical energy storage constraints:

The thermal energy storage and cool storage system constraints are charge and discharge constraints, maximum capacity, and mass balance constraints [28].

Cool storage system maximum capacity:

$$R^{CSS} \le Cap^{CSS} \tag{19}$$

Cool storage system maximum charge and discharge constraints:

$$RDC^{CSS} \le (\vartheta Cap^{CSS}) X^{CSS} \qquad X^{CSS} \in \{0,1\} \tag{20}$$

$$RC^{CSS} \le Cap^{CSS} Y^{CSS} \qquad Y^{CSS} \in \{0,1\} \tag{21}$$

Cool storage system cannot charge and discharge at the same time:

$$X^{CSS}(t) + Y^{CSS}(t) \le 1 \quad \forall\ t\ ,\ X^{CSS}\ and\ Y^{CSS} \in \{0,1\} \tag{22}$$

The thermal energy storage and electrical energy storage constraints are the same as (19) - (22) equations.

D. District heating and cooling network constraints:

The district heating and cooling network minimum and maximum flow constraints can be written as [28]:

$$H_{Min}^{Flow} \le H^{Flow} \le H_{Max}^{Flow} \tag{23}$$

$$R_{Min}^{Flow} \le R^{Flow} \le R_{Max}^{Flow} \tag{24}$$

E. Compression chiller and absorption chiller constraints:

Feasible operating region for absorption chiller and compression chiller units [28]:

$$R_{Min}^{X} \le R^{X} \le R_{Max}^{X} \quad \forall X \in CCH, ACH \tag{25}$$

$$H_{Min}^{X} \le H^{X} \le H_{Max}^{X} \quad \forall X \in CCH, ACH \tag{26}$$

F. Boiler constraints:

The constraints of boilers are [28]:

$$H_{Min}^{B} \le H^{B} \le H_{Max}^{B} \tag{27}$$

G. Heating and cooling loads constraints:

The heating and cooling loads consist of critical and controllable loads [30]. Thus, the controllable heating and cooling loads can be dispatched in the contingent conditions. Hence, the heating and cooling load constraints can be written as:

$$H^{Load} = H_{Critical}^{Load} + H_{Controllable}^{Load} \tag{28}$$

$$\Delta H_{Min}^{DLC} \le \Delta H^{DLC} \le \Delta H_{Max}^{DLC}\ ,\ \Delta H_{Max}^{DLC} = H_{Controllable}^{Load} \tag{29}$$

$$R^{Load} = R^{Load}_{Critical} + R^{Load}_{Controllable} \tag{30}$$

$$\Delta R^{DLC}_{Min} \le \Delta R^{DLC} \le \Delta R^{DLC}_{Max} \;, \Delta R^{DLC}_{Max} = R^{Load}_{Controllable} \tag{31}$$

H. Electric network security constraints:

The apparent power flow limit of lines and voltage limit is given by:

$$\sqrt{P^2(V,\delta)+Q^2(V,\delta)} \le F \tag{32}$$

$$V^{\min} \le |V| \le V^{\max} \tag{33}$$

The apparent power rating of the devices is considered as:

$$\sqrt{P^2+Q^2} \le F^{\max} \tag{34}$$

2.6. The second stage problem

The second-stage problem is a multi-objective optimization problem that minimizes the interruption costs of loads, the mismatch of the operating cost of EGDS resources, and the voltage deviations in the real-time market and the predictive control model is employed as given in [31]. The first objective function of the second stage problem can be formulated as (35):

$$Min\ \mathsf{M} = \sum^{\tau}\sum^{Nzone}\left(\begin{array}{l}\mathbf{Z}|_{\varphi=cte} + \Delta C^{CHP} + \Delta C^{ESS} + \Delta C^{TES} + \Delta C^{CSS} + \Delta C^{DG} + \Delta C^{Boiler} \\ + \Delta C^{ACH} + \Delta C^{CCH} + \Delta C^{DLC} + \Delta C^{PHEVAs} + \Delta C^{TOU} - \Delta revenue \\ \pm \rho^{RT}_{Active}.\Delta P^{Transaction} \pm \rho^{RT}_{reactive}.\Delta Q^{Transaction} + \sum^{NEXSS} prob.ENSC\end{array}\right) \tag{35}$$

$$s.t.: \quad \Xi_2(x,u,z) = 0$$
$$\Omega_2(x,u,z) \ge 0$$

Eq. (32) contains the following parameters: 1) The mismatch of operating cost of CHPs, electrical energy storages, thermal energy storages, cool storage systems, DGs, boilers, absorption chillers, compression chillers, direct load control, PHEVAs, and time-of-use; 2) the mismatch of revenue of energy sold to customers; 3) the active power cost/benefit that is transacted with the upward electricity market; 4) the reactive power cost/benefit that is transacted with the upward electricity market; 5) and the expected ENSCs.

The second stage problem constraints are the same as the first stage problem. Further, the control variables of this problem are the same as the first stage problem.

2.7. The third stage problem

The third stage optimization process implements the on-event corrective actions for the on-outage zones. The zones that are not affected by the extreme shocks are optimally dispatched by the first and second stages in the day-ahead and real-time horizons, respectively.

The external shock segments the zones of EGDS into on-outage and secured zones based on the fact that some of the facilities of on-outage zones may be out of service. Further, the EGDS can switch the electrical switching devices and perform on/off control of the heating/cooling valves of inter-coupling heating and cooling pipelines of neighbour zones.

The control variables of the on-outage zones for the functioning facilities are the same as the first and second stage problem. However, the EGDS can reconfigure its electrical system to perform corrective actions and restore the electrical energy service. The critical loads of on-outage zones should be restored using available DERs, PHEVAs, and demand response aggregators resources. Thus, the third objective function for the on-event corrective actions of on-outage zones can be formulated as (36):

$$
\begin{aligned}
Min\ \mathsf{A} = \mathsf{M} + W_1 * [& \sum^{\tau'} \sum^{NESAzone} \begin{pmatrix} C^{CHP}_{Available} + C^{ESS}_{Available} + C^{TES}_{Available} + C^{CSS}_{Available} + C^{DG}_{Available} + C^{Boiler}_{Available} \\ + C^{ACH}_{Available} + C^{CCH}_{Available} + C^{PHEVAs}_{Available} + C^{DLC}_{Available} + C^{TOU}_{Available} \end{pmatrix} \\
& + \sum^{NSUPzones} \psi^{Switch} . \left(\Delta C^{CHP}_{NSZ} + \Delta C^{ESS}_{NSZ} + \Delta C^{DG}_{NSZ} + \Delta C^{PHEVAs}_{NSZ} + \Delta C^{DLC}_{NSZ} + \Delta C^{TOU}_{NSZ} \right) \\
& + \sum^{NSUPzones} \psi^{DHV} . \left(\Delta C^{CHP}_{NSZ} + \Delta C^{TES}_{NSZ} + \Delta C^{Boiler}_{NSZ} \right) \\
& + \sum^{NSUPzones} \psi^{DCV} . \left(\Delta C^{CHP}_{NSZ} + \Delta C^{CSS}_{NSZ} + \Delta C^{Boiler}_{NSZ} + \Delta C^{ACH}_{NSZ} + \Delta C^{CCH}_{NSZ} \right)] \\
& + W_2 * [\sum^{NESAzone} \sum^{\tau'} (\sum^{NCEL} P^{Load}_{Critical} . IC_{Electrical} + \sum^{NCHL} H^{Load}_{Critical} . IC_{Heating} + \sum^{NCCL} R^{Load}_{Critical} . IC_{Cooling})]
\end{aligned}
\tag{36}
$$

$$
s.t.: \quad \Xi_3^{'}(x,u,z) = 0
$$

$$
\Omega_3^{'}(x,u,z) \geq 0
$$

Eq. (33) consists of two groups of objective functions:

1) The first group of the objective function corresponds to the costs of available CHPs, electrical energy storages, thermal energy storages, cool storage systems, DGs, boilers, absorption chillers, compression chillers, PHEVAs, direct load control, time-of-use, and energy purchased from the upward market costs. This objective function is named as the F_{cost} or first objective function of the third stage problem.

2) The second group of the objective function corresponds to the interruption costs of the electrical, heating and cooling loads. This objective function is named as the $F_{Interruption}$ or second objective function of the third stage problem, while W_1 and W_2 are the weighting factors.

All of the first stage problem constraints are considered for the available facilities, but the minimum and maximum operating values of parameters are changed to their contingency planning values.

The thirds stage optimization process is carried out until the recovery plans and post-event corrective actions such as repairing the damaged facilities is made.

3. Optimization algorithm

Fig. 3 depicts the flowchart of the optimization algorithm, namely:

- The Autoregressive Integrated Moving Average (ARIMA) models are used to generate scenarios for multi-carrier energy loads, day-ahead market prices, real-time market prices, PHEVAs charge/discharge, intermittent electricity generations, and time-of-use electricity consumption.
- Numerous scenarios are generated and the forward selection algorithm is applied to reduce the generated scenarios [32].
- The Monte Carlo stochastic process simulation procedure simulates the external shocks location and intensity [33].
- The linearization of the alternative current load flow is performed using the introduced method of Ref. [34].
- For linearization of ramp-up/down constraints, the algorithm of Ref. [35] is utilized.
- The heating and cooling network constraints are linearized using the algorithm of Ref. [36].
- It is assumed that all of the submitted values of bids/offers of EGDS to upward electricity market are accepted.
- The robust optimization process is utilized to solve the proposed objective function of the first stage problem. The first stage objective function can be rewritten as (37):

$$
\begin{aligned}
Min\ \mathbf{Z} = \sum^{T}\sum^{Nzone}\Bigg(
& C^{CHP}.\varphi^{CHP} + C^{ESS}.\varphi^{ESS} + C^{TES}.\varphi^{TES} + C^{CSS}.\varphi^{CSS} + C^{DG}.\varphi^{DG} \\
& + C^{Boiler}.\varphi^{Boiler} + C^{ACH}.\varphi^{ACH} + C^{CCH}.\varphi^{CCH} + C^{DLC}.\varphi^{DLC} \\
& + \sum^{NPHEVAS} prob.C^{PHEVAs}.\varphi^{PHEVAs} \pm \sum^{NDAMS} prob.\rho^{DA}_{Active}.P^{Transaction}.\varphi^{DA}_{Active} \\
& \pm \sum^{NDAMS} prob.\rho^{DA}_{reactive}.Q^{Transaction}.\varphi^{DA}_{reactive} \pm \sum^{NRTMS} prob.\rho^{RT}_{Active}.P^{Transaction}.\varphi^{DA}_{Active} \\
& \pm \sum^{NRTMS} prob.\rho^{RT}_{reactive}.Q^{Transaction}.\varphi^{DA}_{reactive} + \sum^{TOUS} prob.C^{TOU}.\varphi^{TOU} \\
& + \sum^{NEXSS} prob.ENSC - revenue + (\gamma^{-R}P^{R} + u'] + \Theta\Gamma
\Bigg)
\end{aligned}
\tag{37}
$$

$$
\begin{aligned}
s.t.:\ & \Xi_1(x,u,z) = 0 \\
& \Omega_1(x,u,z) \geq 0 \\
& \Theta + u' \geq \xi\nu \\
& u' \geq 0 \\
& \nu \geq 0 \\
& -\nu \leq P^{R} \leq \nu \\
& \Theta \geq 0
\end{aligned}
$$

- The mixed-integer problem is solved using the mixed-integer programming solver of GAMS.
- The ARIMA forecasting model with the 1-minute resolution is used for the second stage problem.
- The linearized model is solved using the CPLEX solver of GAMS.
- The third stage optimization problem is solved using the mixed-integer linear programming solver of GAMS.

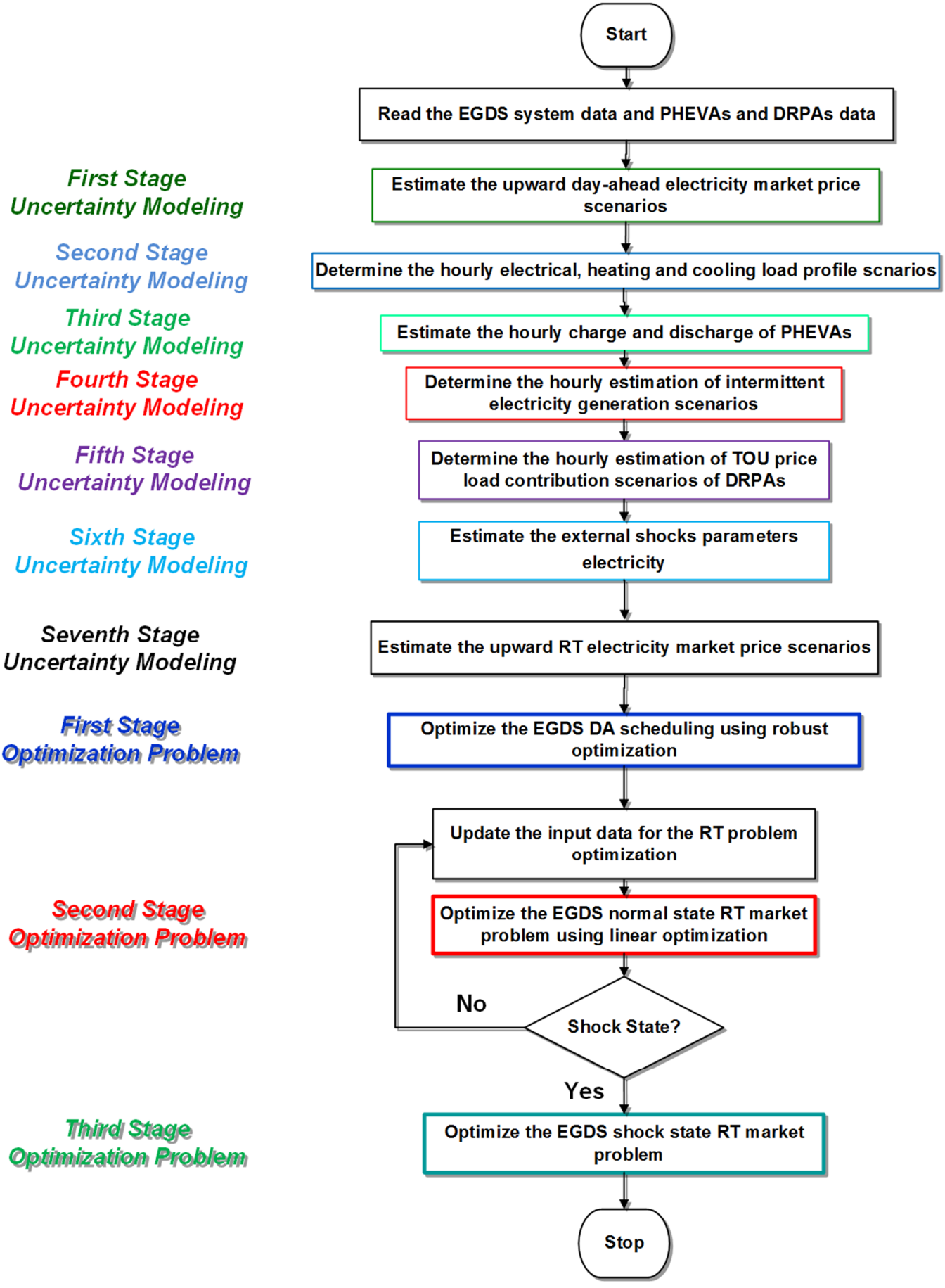

Fig. 3. The overall flowchart of the proposed OROS procedure.

4. Simulation Results

The 123-bus test system was used to assess the proposed framework. The 123-bus test system topology is shown in Fig. 4. Table 3 depicts the parameters of scenario generation and reduction for the 123-bus system. The topology of district heating and cooling system of each zone is the same as the electrical system of the corresponding zone. The district heating and cooling systems of each zone are connected to the neighbour zones through on/off control valves that can be controlled in extreme shock conditions to mitigate the impacts of shocks.

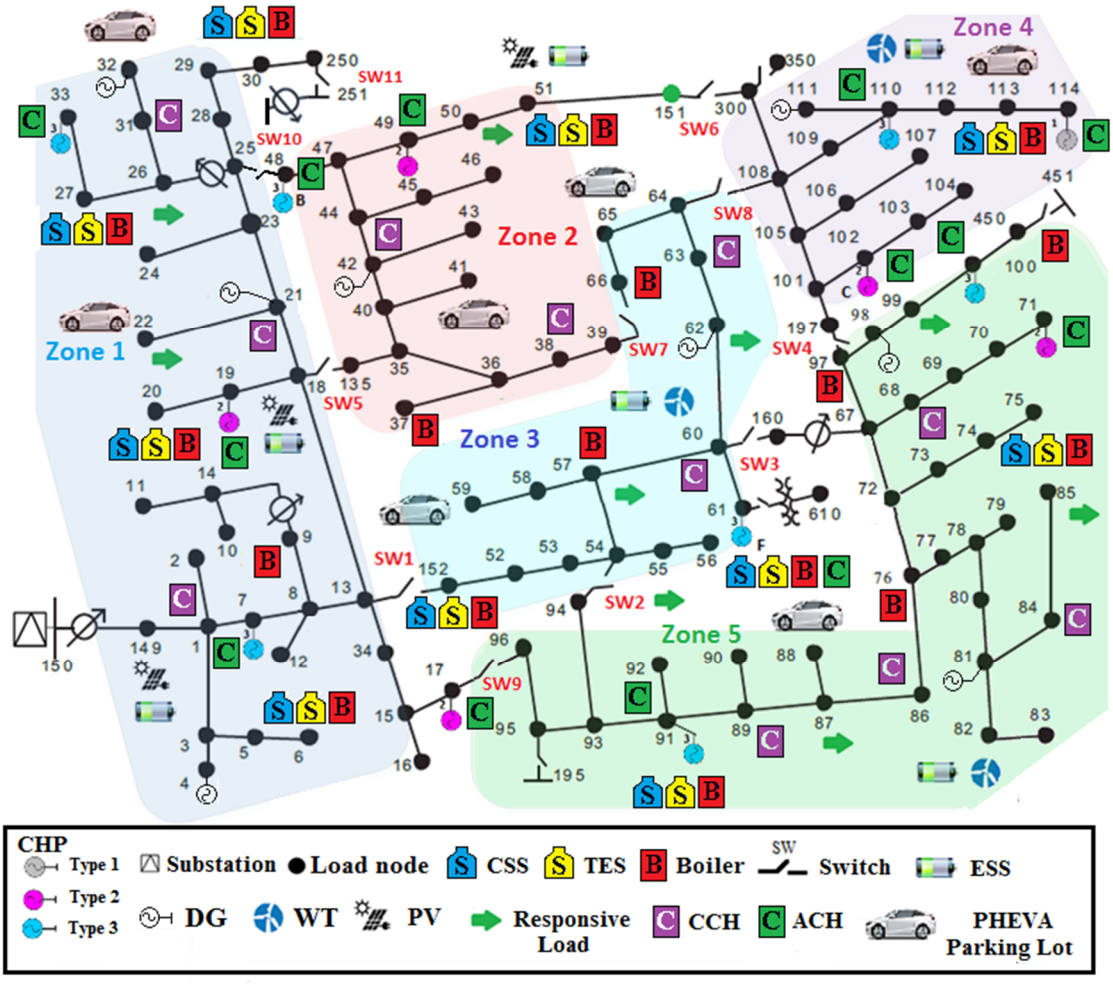

Fig.4. The modified 123-bus EGDS test system.

Fig. 5 depicts the estimated electrical, heating and cooling load for one of the reduced scenarios. The day-ahead hourly heating, cooling and electrical loads were estimated by the ARIMA models [37]. The per-unit load hourly electrical, heating and cooling load profiles of Ref. [38] were used to generate the base per unit hourly load profiles. Different scenarios of weather conditions were considered and the hourly load profiles were generated. Then, a scenario reduction process was utilized to find the day-ahead hourly load profiles [38]. The forecasted electrical loads were delivered to the price-forecasting machine of Ref. [39] and the day-ahead hourly price of energy and ancillary services were forecasted. Fig. 6 depicts the estimated values of the upward electricity market prices.

Table 3. The optimization input data for the 123-bus system.

System parameter	Value
Number of solar irradiation scenarios	1500
Number of wind turbine power generation scenarios	1500
Number of PHEVAs contribution scenarios	1500
Number of demand response aggregators contribution scenarios	1500
Number of solar irradiation reduced scenarios	15
Number of wind turbine power generation reduced scenarios	15
Number of PHEVAs contribution reduced scenarios	15
Number of demand response aggregators contribution reduced scenarios	15

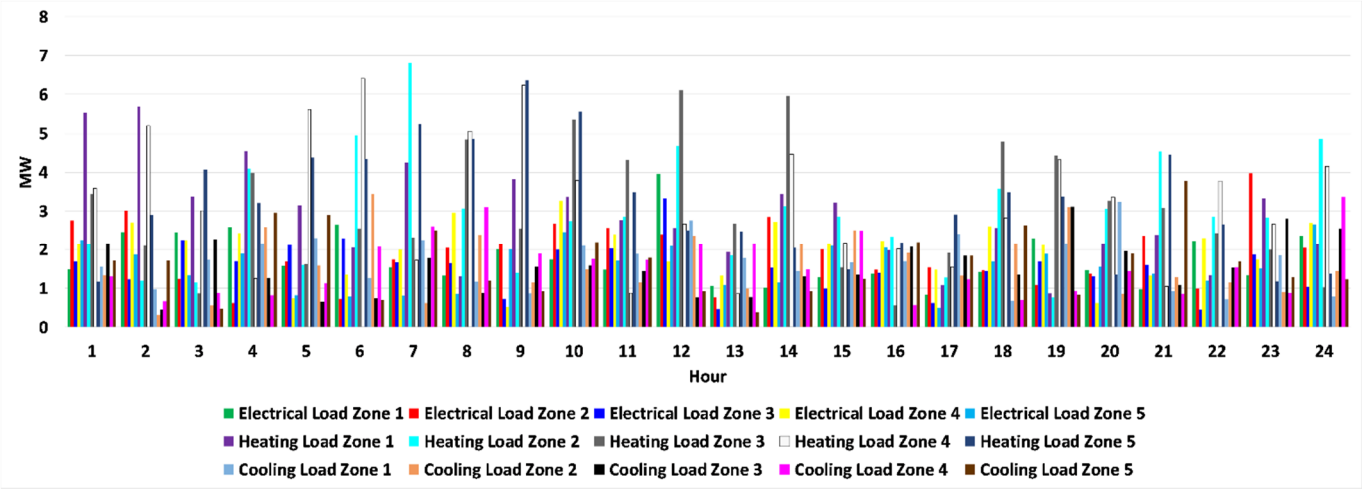

Fig. 5. The estimated 123-bus system electrical, heating and cooling load of zones for one of the reduced scenarios.

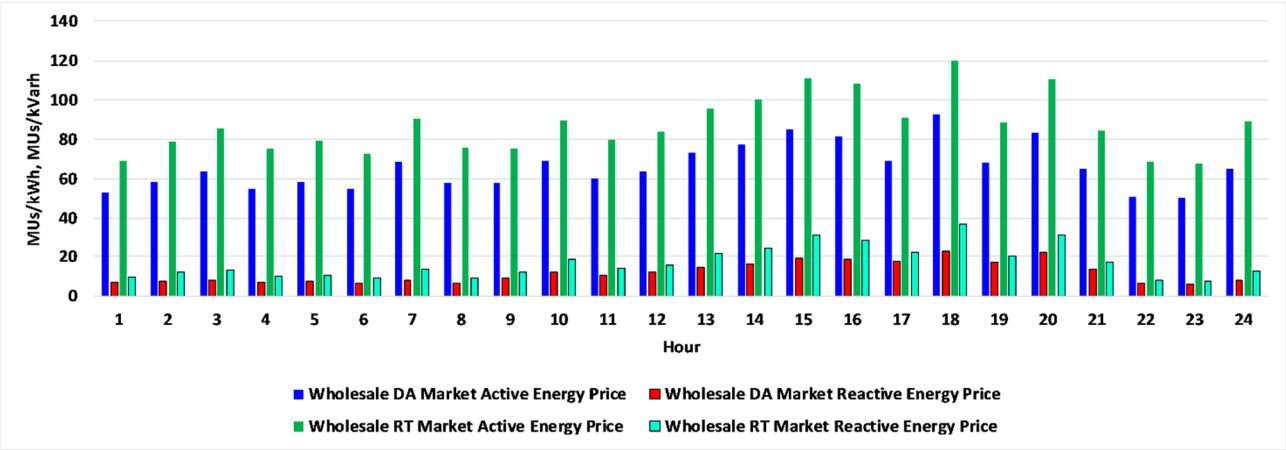

Fig. 6. The estimated value of active and reactive power prices.

Fig. 7 presents the estimated values of photovoltaic systems and wind turbines electricity generations. The wind turbines and photovoltaic electricity generations are functions of solar irradiation and wind speed, respectively. The detailed model of wind turbines and photovoltaic electricity generations are presented in [40] and [41], respectively. The ARIMA models were used to generate scenarios for solar irradiation and wind speed. The photovoltaic systems and wind turbines facilities were equipped with the electrical storage systems. Thus, these facilities were considered as dispatchable distributed generation facilities.

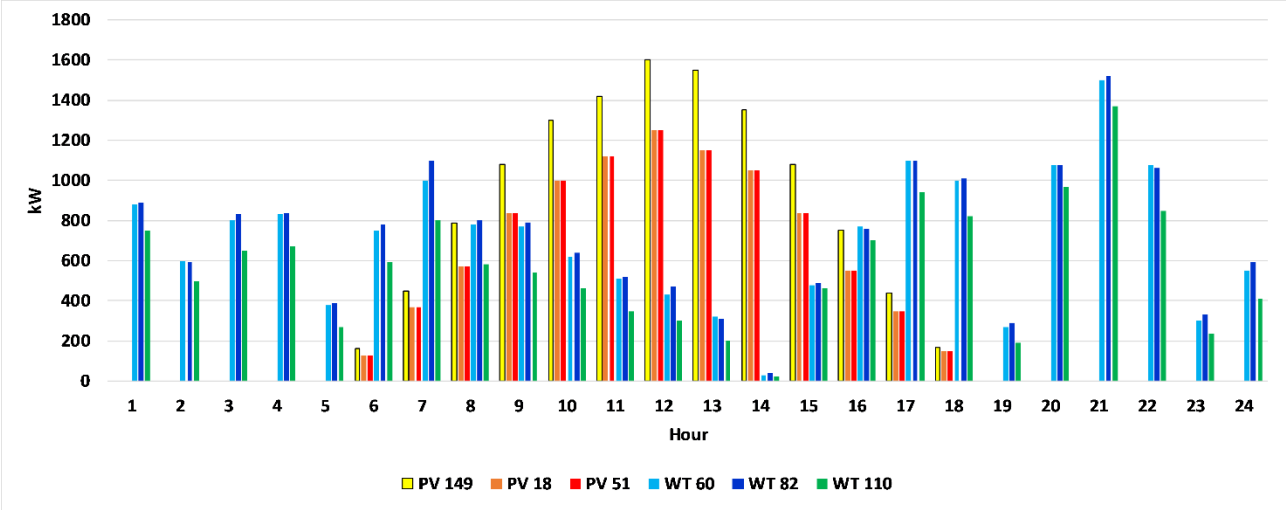

Fig. 7. The estimated value of photovoltaic systems and wind turbines electricity generations for one of the reduced scenarios.

Table 4 and Table 5 present the input parameters of the simulation and the load interruption costs, respectively. As mentioned earlier, it was assumed that the EGDS system was segmented into different zones such that each zone was adequately designed to tolerate the expected and routine external shock levels and the N-1 system contingencies [9]. Fig. 8 depicts the maximum value of hourly interruption costs of electrical, heating and cooling loads for different zones of the EGDS.

Table 4. The input parameters of simulation process.

	Parameters		
CHP	Type 1	Type 2	Type 3
	0.12 kW fuel consumption (m^3/kWh)=0.282	0.25 kW fuel consumption (m^3/kWh)=0.273	0.33 kW fuel consumption (m^3/kWh)=0.269
PhotoVoltaic system (PV)	Maintenance cost =15 MUs/kWh		
	Photovoltaic arrays aggregated capacity (for 18, 51, and 149 bus)= 2 MW		
Wind Turbine (WT)	Maintenance cost=25 MUs/kWh, Wind turbine aggregated capacity for 60, 82, and 110 bus= 1800 kW		
Fossil fuelled DG	1200 kW, fuel consumption (m^3/kWh)=0.336		
Absorption CHiller (ACH)	Maintenance cost ACH (0.4 MW) =1.2 MUs/kWh, COP=0.8, Maintenance cost ACH (0.48 MW) =14.5 MUs/kWh, COP=0.81, ACH (114,17,49,19,71,102)=400 kW, ACH(7,33,48,61,91,100,110) =480 kW		
Compression CHiller (CCH)	Maintenance cost =1.4 MUs/kWh, COP=4, Capacity=400 kW		
Electrical Storage System (ESS)	Modules capacity= 100 kW, Type: Lead-acid battery, Efficiency=0.75, Maintenance cost (ESS)=0.54 MUs/kWh		
Thermal Energy Storage (TES) and Cool Storage System (CSS)	Maintenance cost (TES)=38 MUs/kWh, Maintenance cost (CSS)=30 MUs/kWh, CSS modules capacity= 100 kW, CSS type (ice storage), TES modules capacity= 100 kW, TES type (hot water storage)		
Boiler	Maintenance cost =13 MUs/kWh		
Natural gas fuel price	44 MU/kWh		
PHEV	Minimum PHEVs energy = 4 kWh, Maximum PHEVs energy = 18 kWh		

Table 5. The electrical, heating and cooling load interruption costs [28].

Parameter	Price	Parameter	Price
Average electrical load interruption costs zone 1,4,5(MMUs/MWh)	0.42	Average electrical load interruption costs zone 2, 3(MMUs/MWh)	0.38
Average heating load interruption costs zone 1,4,5(MMUs/MWh)	0.25	Average heating load interruption costs zone 2, 3(MMUs/MWh)	0.34
Average cooling load interruption costs zone 1,4,5(MMUs/MWh)	0.18	Average cooling load interruption costs zone 2, 3(MMUs/MWh)	0.26
λ^{active}	$1.2 * \rho_{Active}$	$\lambda^{heating}$	$0.7 * \lambda^{active}$
$\lambda^{reactive}$	$1.2 * \rho_{Active}$	$\lambda^{cooling}$	$0.8 * \lambda^{active}$

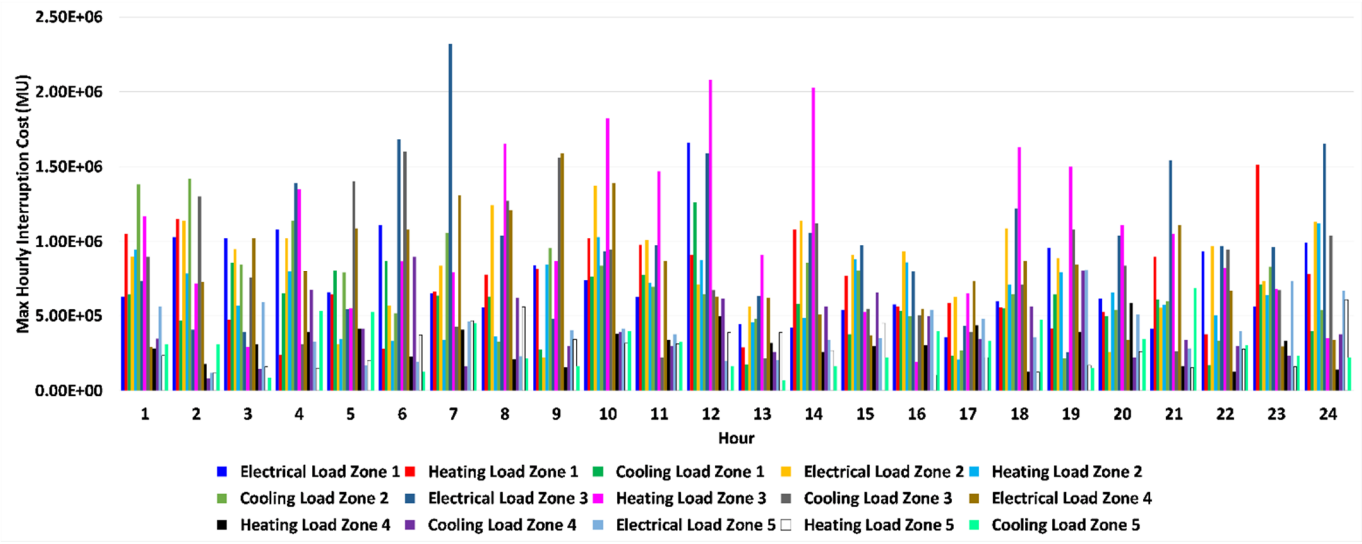

Fig. 8. The maximum value of hourly interruption costs of critical electrical, heating and cooling loads for zones.

4.1. First stage problem simulation outputs

The simulation of the proposed algorithm was carried out for different values of Γ parameter. Fig. 9. (a) and (b) present the stacked column of the estimated optimal electricity and heating outputs for Γ=0, respectively.

Fig.10 depicts the stacked column of the estimated optimal DGs outputs, PHEVAs, electrical energy storages dispatch, and electrical load after demand response program implementation for Γ=0. The DGs tracked the electrical load and the PHEVAs and electrical energy storages were committed by the EGDS as dispatchable resources to supply the electrical load of the system. The electrical load was optimally controlled and the EGDS transacted energy with the upward electricity market in day-ahead horizon.

Fig. 11 presents the stacked column of the estimated optimal boilers dispatch for Γ=0. The boilers tracked the heating load to supply it.

Fig. 12. (a), (b) present the stacked column of the estimated optimal absorption chillers and compression chillers dispatch for Γ=0, respectively. The absorption chillers supplied cooling load and their outputs were dependent on the CHPs heating energy outputs.

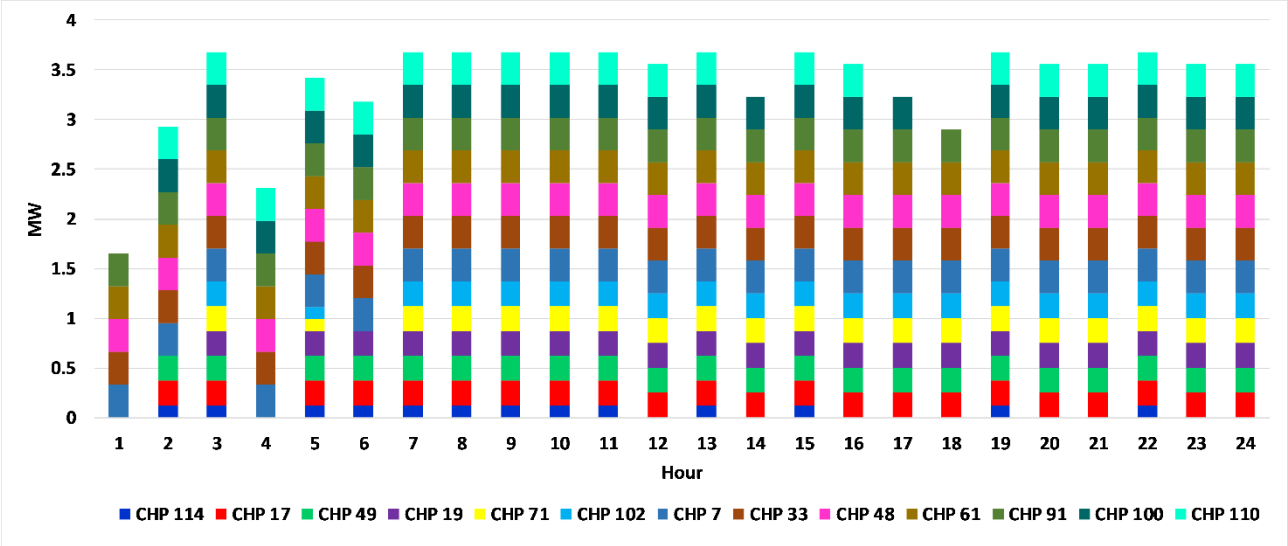

(a)

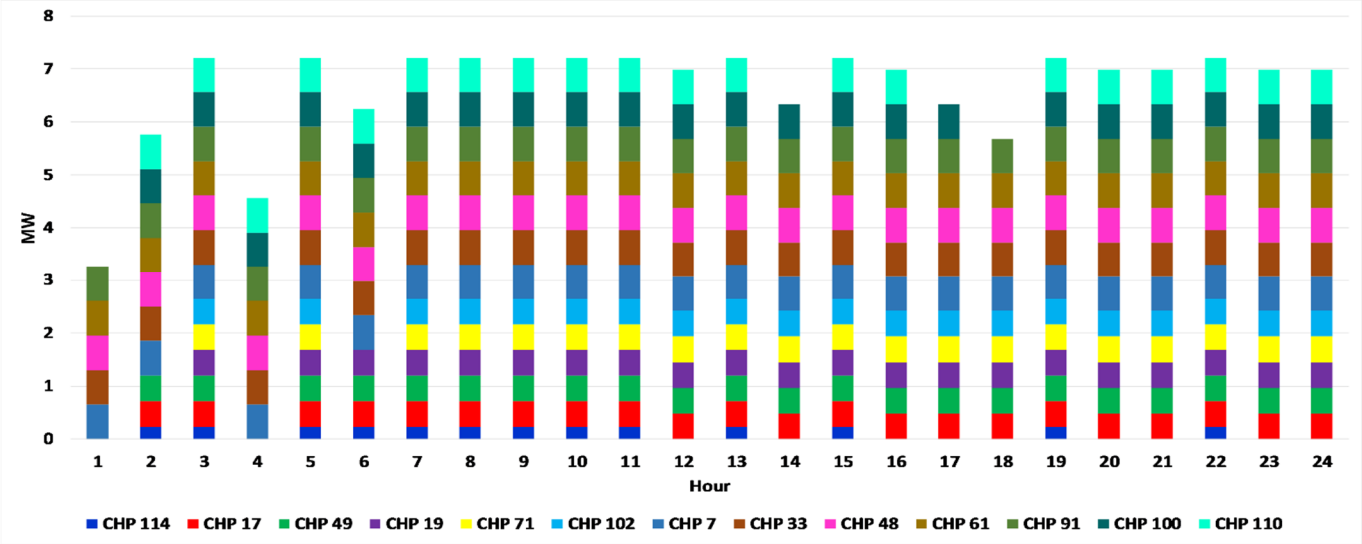

(b)

Fig. 9. (a) The stacked column of the estimated optimal CHPs electricity outputs for Γ=0. (b) The stacked column of the estimated optimal CHPs heating energy outputs for Γ=0.

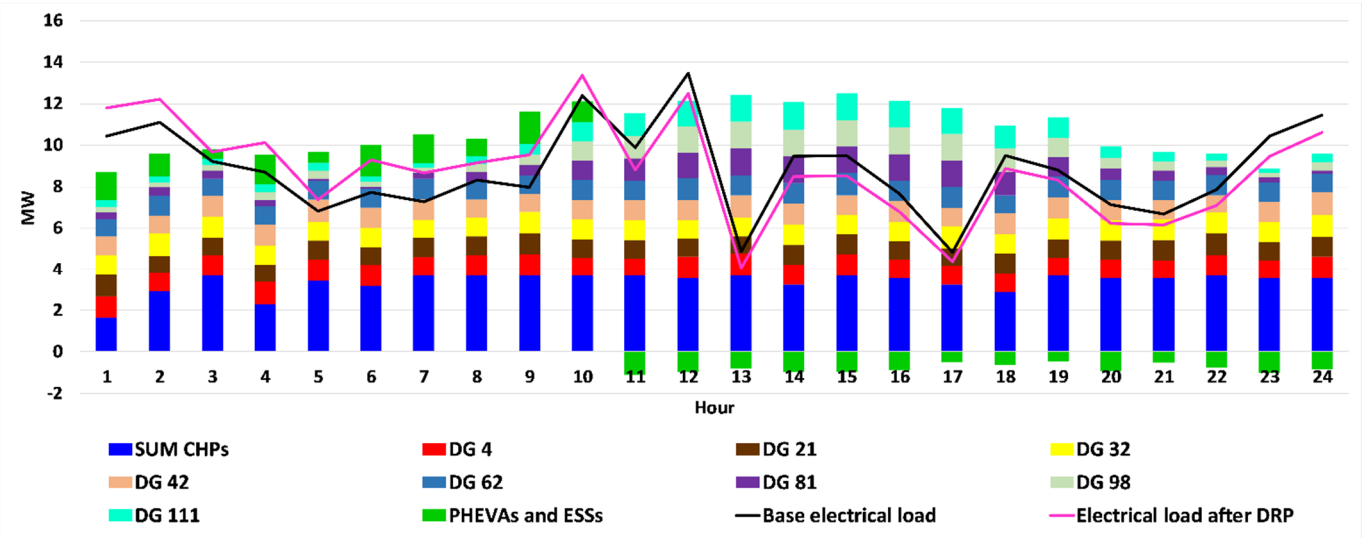

Fig.10. The stacked column of the estimated optimal DGs outputs, PHEVAs and electrical energy storages dispatch and electrical load after demand response program implementation for Γ=0.

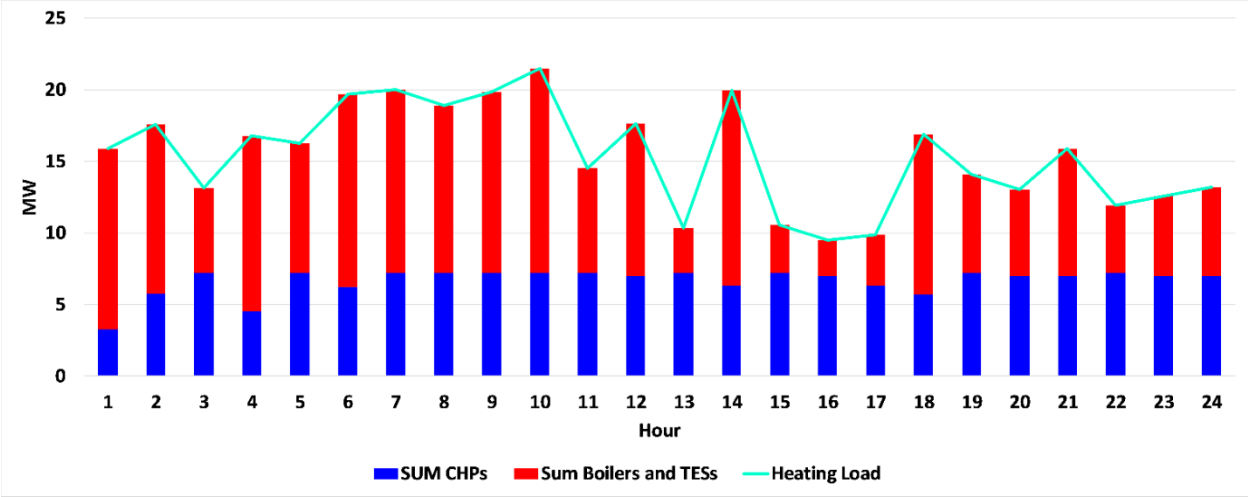

Fig. 11 The stacked column of the estimated optimal boilers dispatch for Γ=0.

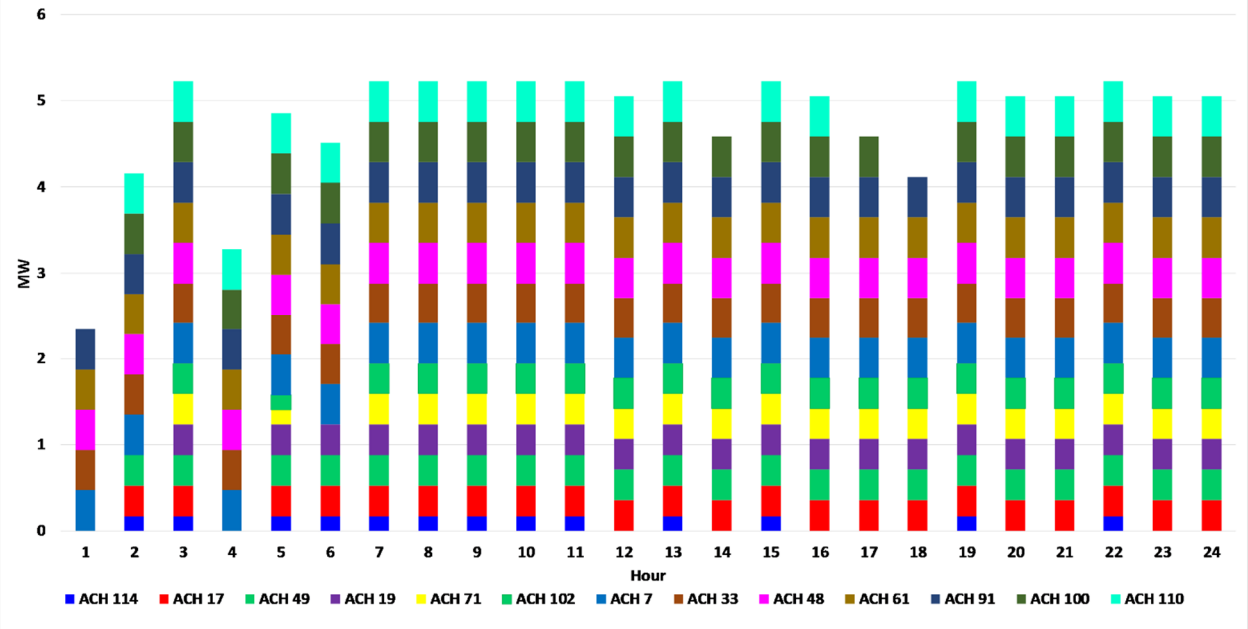

(a)

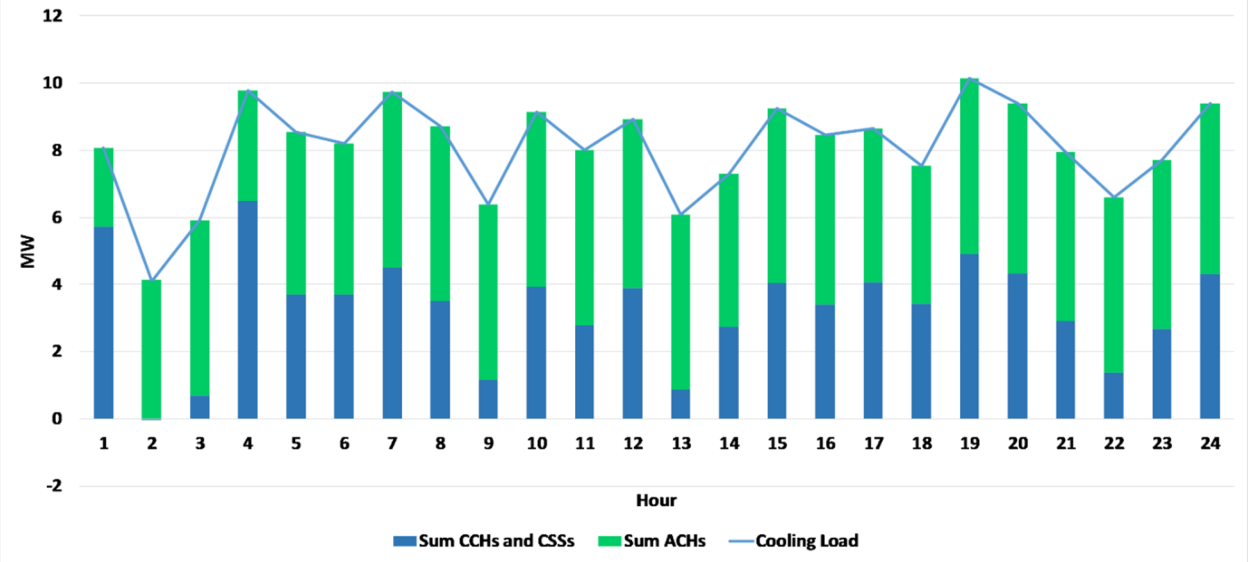

(b)

Fig. 12 (a) The stacked column of the estimated optimal absorption chillers dispatch for Γ=0. (b) The stacked column of the estimated optimal compression chillers dispatch for Γ=0.

Fig. 13 presents the stacked column of the estimated optimal thermal energy storages, cool storage systems, and PHEVAs dispatch for Γ=0, respectively in (a), (b) and (c). The thermal energy storages and cool storage systems were optimally dispatched to supply the heating and cooling loads. Further, the PHEVAs were utilized to reduce the electrical peak load and increase the electrical load of off-peak hours.

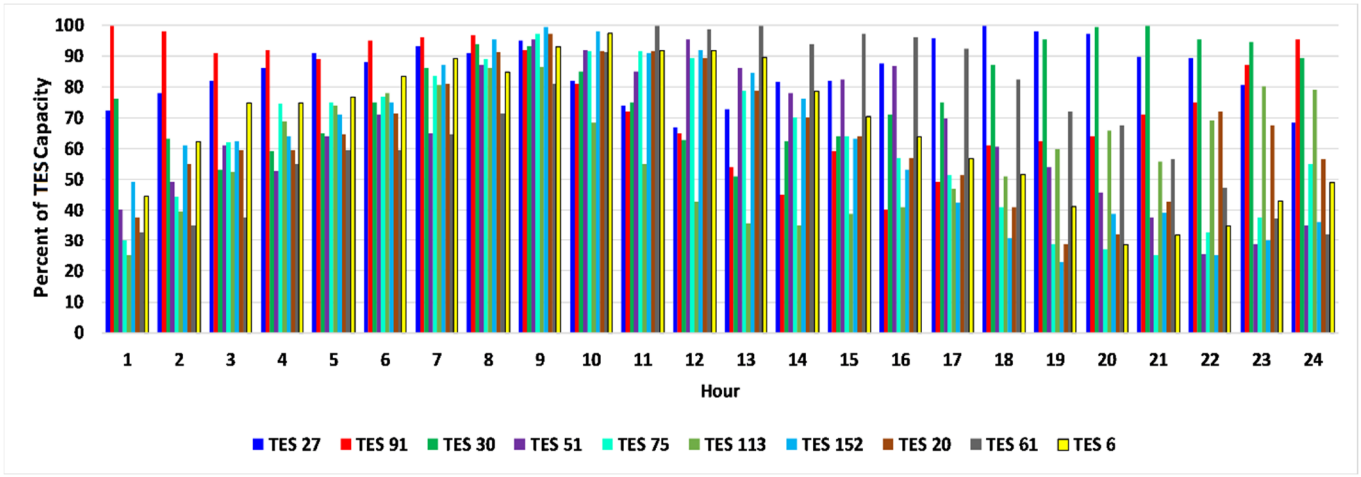

(a)

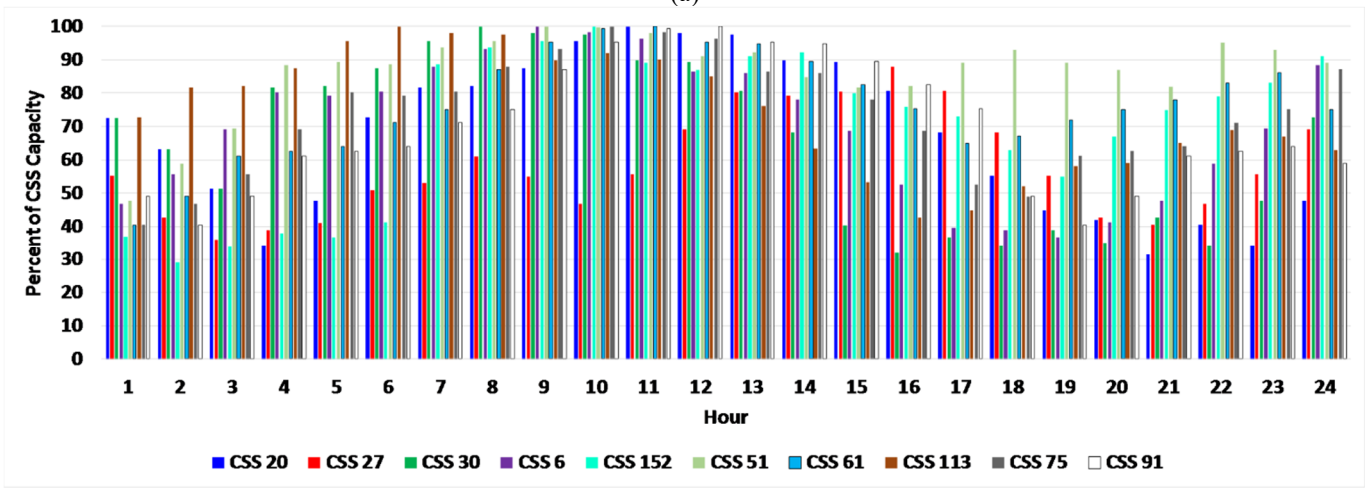

(b)

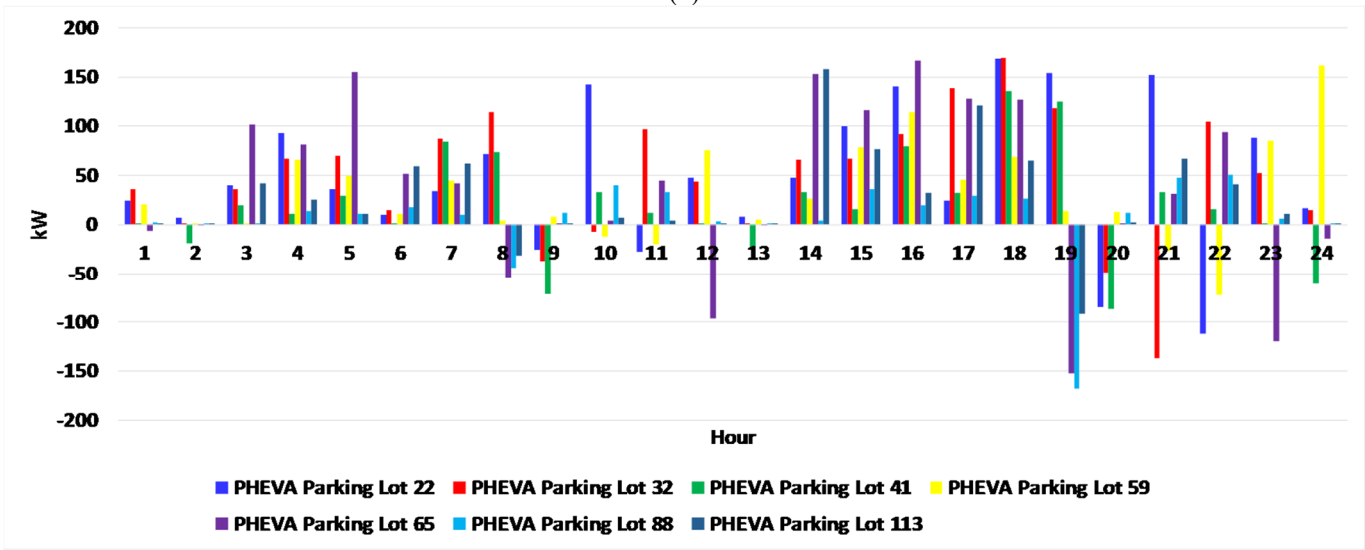

(c)

Fig. 13. (a) The stacked column of the estimated optimal thermal energy storages dispatch for Γ=0. (b) The stacked column of the estimated optimal cool storage systems dispatch for Γ=0, (c) The stacked column of the estimated optimal PHEVAs dispatch for Γ=0.

Fig. 14 depicts the values of the EGDS active and reactive power generation, day-ahead electricity transactions with the upward market, and electrical load after demand response program implementation for different values of Γ.

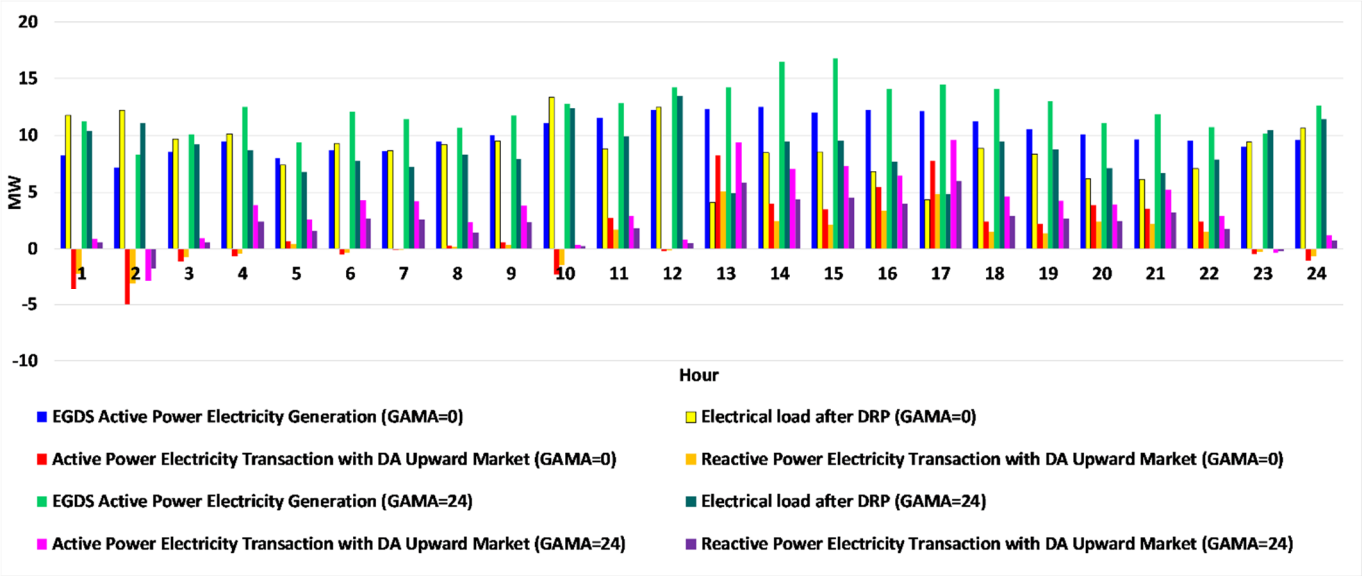

Fig. 14. The values of the EGDS active and reactive power generation, day-ahead electricity transactions with the upward market, and electrical load after demand response program implementation for different values of Γ.

The estimated values of the EGDS active electrical energy generation for Γ=0 and Γ=24 were 244.153 MWh and 297.166 MWh. respectively. Thus, the EGDS generated more electrical energy for the Γ=24 condition, even when the electricity prices of the upward market were lower than its electricity generation costs. The estimated energy consumption of electrical loads were 211.390 MWh and 211.394 MWh for Γ=0 and Γ=24 values, respectively. The EGDS utilized demand response programs and energy storage devices to change the multi-energy carriers load profiles. However, the estimated electrical energy consumptions were equal for both Γ=0 and Γ=24 conditions. The net transacted active energy between EGDS and upward electricity market were 32.763 MWh and 85.772 MWh for Γ=0 and Γ=24, respectively. Fig. 15 (a) and (b) depict the estimated values of the active/ reactive markets cost/ benefit of the EGDS for the day-ahead and real-time markets and the total costs of the EGDS for different values of Γ, respectively. The estimated values of total day-ahead active and reactive costs of the EGDS were 2.721 MMUs and 0.420 MMUs for Γ=0, respectively. Further, the estimated values of total real-time active and reactive costs of the EGDS were 1.23 MMUs and 0.210 MMUs for Γ=0, respectively. The estimated values of total day-ahead active and reactive costs of the EGDS were 6.299 MMUs and 0.832 MMUs for Γ=24, respectively. Further, the estimated values of total real-time active and reactive costs of the EGDS were 0.987 MMUs and 0.142 MMUs for Γ=24, respectively. As shown in Fig. 15, the EGDS cost was increased for Γ=24 and the system reduced its transactions with the upward market in real-time market to manage the economic risk. Further, the EGDS cost was increased for greater values of Γ based on the fact that the EGDS selected the risk-averse strategy.

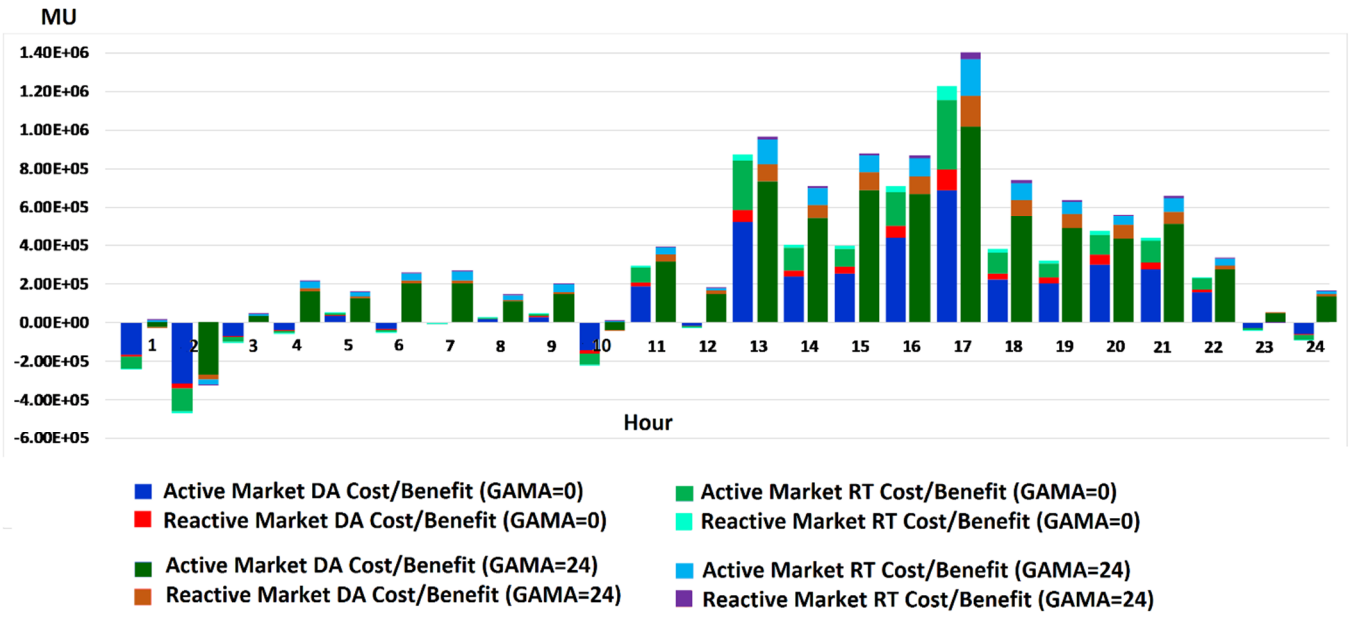

(a)

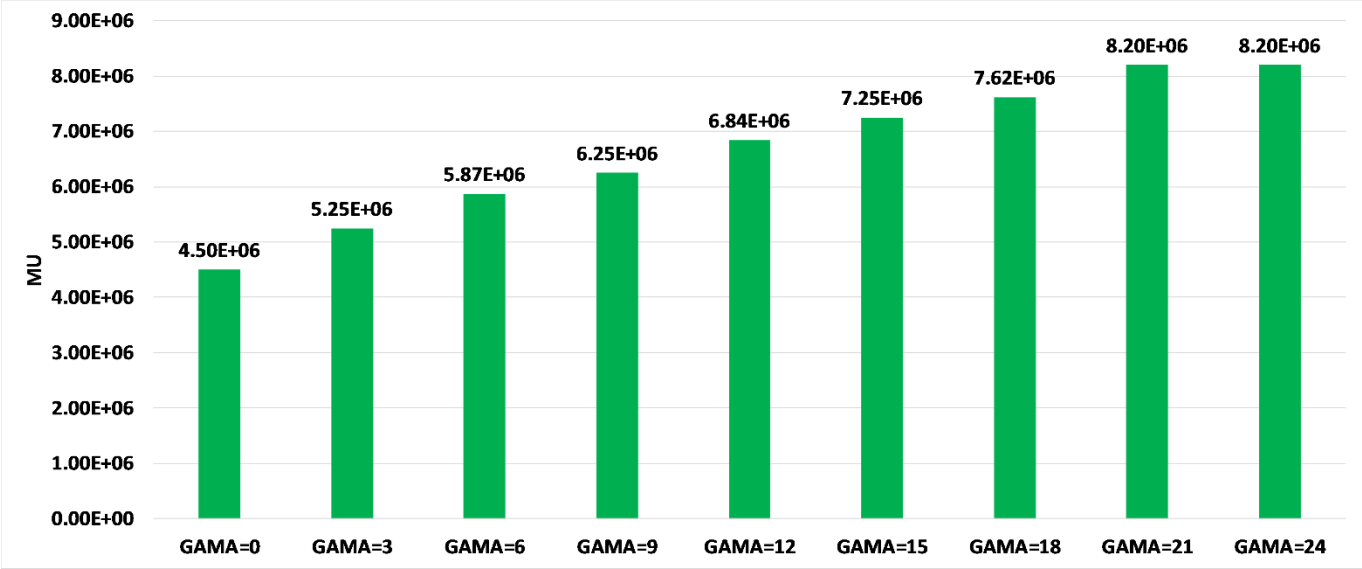

(b)

Fig. 15. (a) The estimated values of the active/ reactive markets cost/ benefit of the EGDS for the day-ahead and real-time markets and for different values of Γ. (b) The total costs of the EGDS for different values of Γ.

4.2. Second stage problem simulation

The load and price data were updated and delivered to the second stage problem. Fig. 16 presents the estimated values of first and second stage objective functions for different values of input parameters. The estimated values of the first stage problem active and reactive real-time electrical energy transactions were 11.572 MWh and 7.169 MVARh for Γ=0, respectively. Further, the estimated values of the first stage problem active and reactive real-time electrical energy transactions were 10.433 MWh and 6.643 MVARh for Γ=24, respectively. Thus, the EGDS transacted less energy with the real-time upward electricity market for risk-averse conditions.

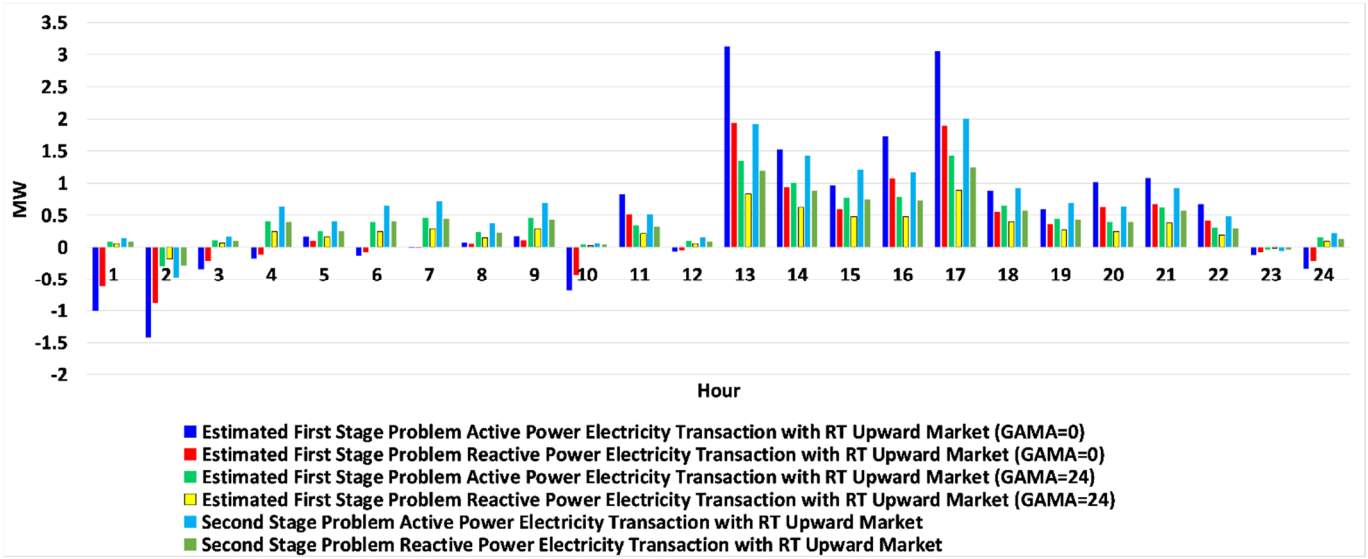

Fig. 16. The estimated values of first and second stage objective functions for different values of input parameters.

The values of the second stage problem active and reactive real-time electrical energy transactions were 15.579 MWh and 9.652 MVARh, respectively. The mismatches of the transacted active energy were 34.62% and 43.32% for Γ=0 and Γ=24, respectively. The high value of mismatch presented the volatility of multiple stochastic input parameters. The extreme shock impacts on the system and the simulation of corrective actions are considered in the next subsection.

By comparing Fig. 14 and Fig. 16, it can be concluded that the EGDS increased the multi-carrier energy generation by its own facilities for the risk-averse strategy. However, the EGDS operational costs were increased for the risk-averse strategy based on the fact that the system transacted less electricity with the real-time electricity market and utilized the expensive electricity generation devices when the upward electricity prices were lower than the marginal costs of its facilities.

4.3. Third stage problem simulation outputs

The simulation of the impact of extreme shocks on the EGDS system was carried out for the described cases. Table 6 shows the EGDS optimal switching of electrical switches and on/off control of district heating and cooling line valves for the 25 top external shock conditions and the results were determined by the third stage optimization process. The total number of simulated external shock was 600 and the output of the simulation for each case was stored. The weighting factors were assumed equal to 1.

Fig. 17 shows the maximum expected value of the hourly first objective function of third stage problem (F_{cost}) for different values of Γ that was determined in the third stage problem for all of the considered external shock scenarios. The maximum value of *Fcos*t took on a value 1.237 MMUs for Γ=24, and hour=18. The minimum value of *Fcos*t took on a value 0.02519 MMUs for Γ=0, and hour=7.

Table 6. The EGDS optimal switching of electrical switches and on/off control of district heating and cooling line valves for the 25 top external shock conditions

			Number of Switch/District Heating Control Valve/District Cooling Control Valve										
External Shock Region	Zone	External Shock Number	1	2	3	4	5	6	7	8	9	10	11
13-18	1	1	ON	OFF	ON	ON	ON	OFF	ON	ON	OFF	OFF	OFF
13-34	1	2	ON	OFF	ON	ON	ON	OFF	OFF	OFF	ON	OFF	OFF
18-21	1	3	ON	OFF	ON	ON	ON	OFF	OFF	OFF	OFF	ON	OFF
25-28	1	4	ON	OFF	ON	ON	ON	OFF	OFF	OFF	OFF	OFF	ON
13-8	1	5	OFF	OFF	ON	ON	ON	ON	OFF	ON	ON	OFF	OFF
135-35	2	6	ON	OFF	ON	ON	OFF	OFF	OFF	OFF	OFF	OFF	OFF
49-50	2	7	ON	OFF	ON	ON	ON	ON	OFF	OFF	OFF	OFF	OFF
40-42	2	8	ON	OFF	ON	ON	ON	ON	OFF	OFF	OFF	OFF	OFF
51-151	2	9	ON	OFF	ON	ON	ON	ON	OFF	OFF	OFF	ON	OFF
36-38	2	10	ON	OFF	ON	ON	ON	OFF	OFF	OFF	OFF	OFF	OFF
54-57	3	11	ON	ON	ON	ON	ON	OFF	OFF	OFF	OFF	OFF	OFF
60-62	3	12	ON	OFF	ON	ON	ON	OFF	ON	ON	OFF	OFF	OFF
57-60	3	13	ON	ON	ON	ON	ON	OFF	OFF	OFF	ON	OFF	OFF
63-64	3	14	ON	OFF	ON	ON	ON	OFF	OFF	ON	OFF	OFF	OFF
152-52	3	15	ON	ON	ON	ON	ON	OFF	OFF	OFF	OFF	OFF	OFF
101-105	4	16	ON	OFF	ON	ON	ON	ON	OFF	OFF	OFF	OFF	OFF
105-108	4	17	ON	OFF	ON	ON	ON	ON	OFF	OFF	OFF	OFF	OFF
107-97	4	18	ON	OFF	ON	ON	ON	ON	OFF	OFF	ON	OFF	OFF
101-102	4	19	ON	OFF	ON	ON	ON	OFF	OFF	OFF	OFF	OFF	OFF
109-110	4	20	ON	OFF	ON	ON	ON	OFF	OFF	OFF	OFF	OFF	OFF
72-76	5	21	ON	ON	ON	ON	ON	OFF	OFF	OFF	OFF	OFF	OFF
86-87	5	22	ON	ON	ON	ON	ON	OFF	OFF	OFF	OFF	OFF	OFF
72-67	5	23	ON	ON	ON	ON	ON	OFF	OFF	OFF	OFF	OFF	OFF
80-81	5	24	ON	OFF	ON	ON	ON	OFF	OFF	OFF	OFF	OFF	OFF
93-91	5	25	ON	ON	ON	ON	ON	OFF	OFF	OFF	OFF	OFF	OFF
Normal	----	----	ON	OFF	ON	ON	ON	OFF	OFF	OFF	OFF	OFF	OFF

OFF ON

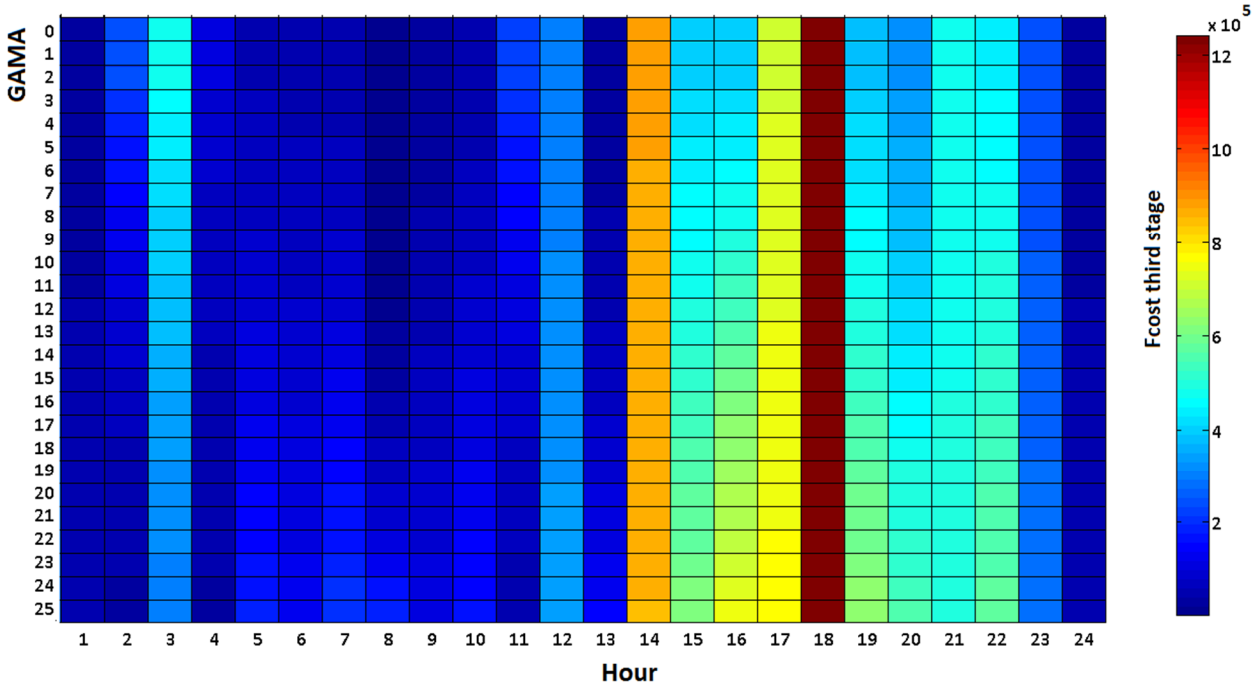

Fig. 17. The maximum expected value of the hourly first objective function of third stage problem (F_{cost}) for different values of Γ that was determined in the third stage problem for all of the considered external shock scenarios.

Fig. 18 (a) shows the expected values of the hourly optimal objective function of third stage problem ($F_{cost} + F_{Interruption}$) for the 600 cases of the considered external shock scenarios and optimal values of Γ. The proposed algorithm determined the optimal value of Γ for the probable external shock. The maximum value of the objective function of the third stage problem took on a value 2.263 MMUs for external shock=411, Γ=14, and hour=12. This credible external shock condition is explored in the next paragraphs. The minimum value of the objective function of third stage problem took on a value 0.09051 MMUs for external shock=54, Γ=0, and hour=0.

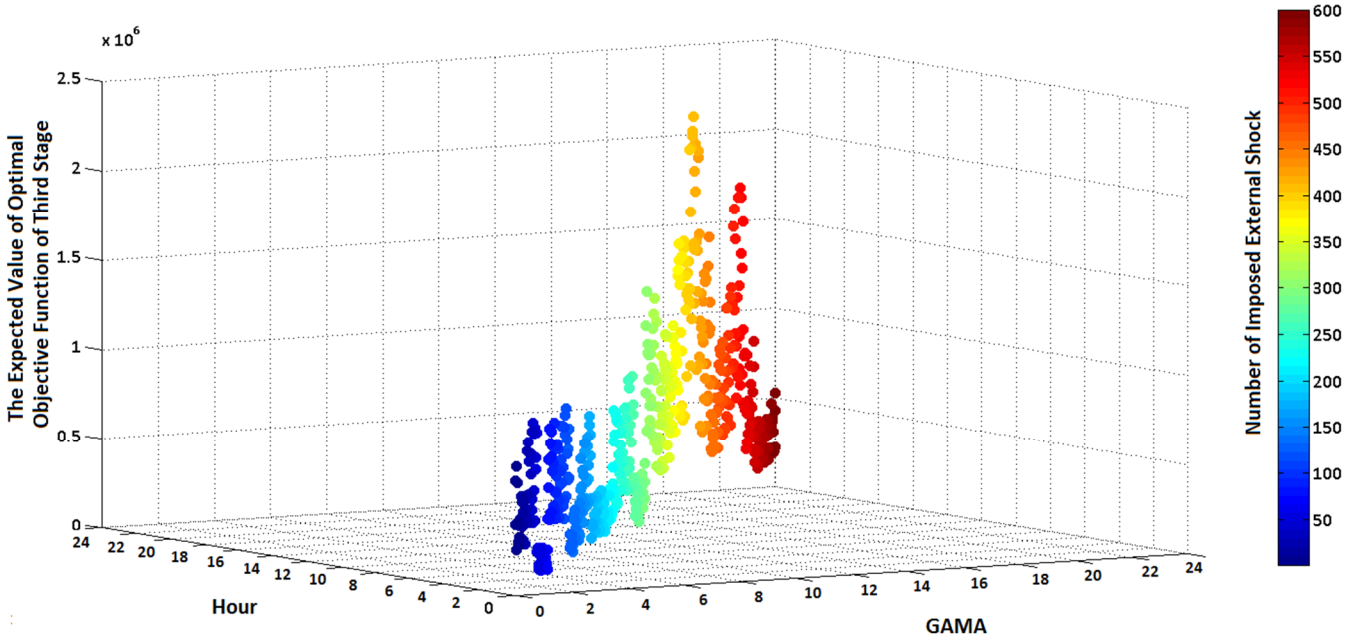

(a)

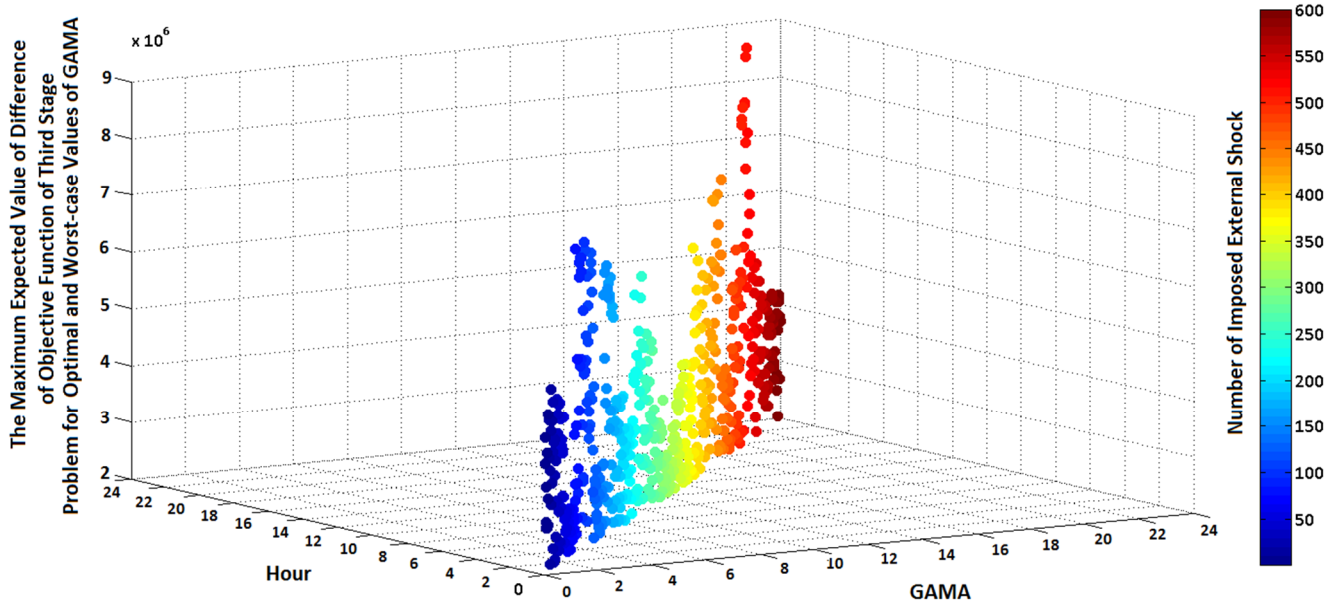

(b)

Fig. 18. (a). The expected values of the hourly optimal objective function of third stage problem for optimal values of Γ and 600 cases of the considered external shock scenarios. (b) The expected values of the difference of objective function of non-performed and performed corrective actions of the third stage problem.

For assessing the effectiveness of the corrective actions, two cases were considered and their results were analysed: 1) the overall OROS with the proposed corrective actions was performed, and 2) only the load shedding process was performed and the OROS procedure was considered without the proposed corrective actions.

Fig. 18 (b) shows the differences of the expected values of objective function of non-performed and performed corrective actions of the third stage problem for the considered external shock scenarios. The maximum value of Fig. 18 (b) took on a value of 8.909 MMUs that was for external shock=411, Γ=14, and hour=12. This value was the difference of the objective function of non-performed and performed corrective actions for the third stage problem. Thus, the OROS reduced the expected cost of the system by about 74.59% for the external shock=411, Γ=14, and hour=12. The minimum value of Fig. 18 (b) took on a value 2.120 MMUs that was for external shock=54, Γ=0, and hour=0. By comparing Fig. 18 (a) and Fig. 18 (b) for the different external shocks, it can be concluded that the corrective actions of the third stage problem of OROS reduced the aggregated expected value of the objective functions of third stage problem by about 57.73% for all of the 600 cases of the considered external shock scenarios.

The external shock 411 was one of the worst-case scenarios of external shocks and the following facilities were out of service for four hours for this shock:

- Triple lines of the first zone (line 18-21, line 21-23, line 23-25),
- Triple lines and one CHP of the second zone (line 47-49, line 49-50, line 50-51, CHP bus 49),
- Triple lines and two buses of the fifth zone (line 76-86, line 86-87, line 87-89, bus 88 and bus 90).

The EGDS run the third stage optimization problem and determined the optimal switching of electrical switches and on/off control of district heating and cooling line valves for the defined external shock. Further, the optimal on-event dispatch of system resources was determined.

Fig. 19 (a), (b), (c), (d) depict the third stage corrective actions simulations outputs for the optimal pre-event and on-event dispatch values of CHPs, thermal energy storages, cool storage systems, and PHEVAs, respectively. The CHPs of EGDS were fully committed and the DGs of the system tracked the electrical load of the EGDS. As shown in Figs. 19 (b), (c) the thermal energy storages and cool storage systems compensated any mismatch between heating and cooling generations and consumptions. Further, the PHEVAs' parking lots were utilized to supply the critical electrical loads in post-event conditions.

Fig. 20 depicts the estimated pre-event and on-event dispatch of district heating and cooling pipelines of zone 2-zone 1 and zone 4- zone 2. The district heating and cooling valves were opened and energy carriers were transferred to the external shock affected zones.

Fig. 21 (a), (b), (c) depict the estimated pre-event and on-event electrical load, heating load, and cooling load for the external shock affected zones, respectively. The demand response aggregator contributions reduced the electrical loads of the zones for post-event conditions as shown in Fig. 21 (a). The maximum values of estimated electrical load reduction procured by the demand response aggregator were 1.007 MW (zone 1 for hour 12), 0.9191 MW (zone 2 for hour 12) and 0.742 MW (zone 5 for hour 19), respectively.

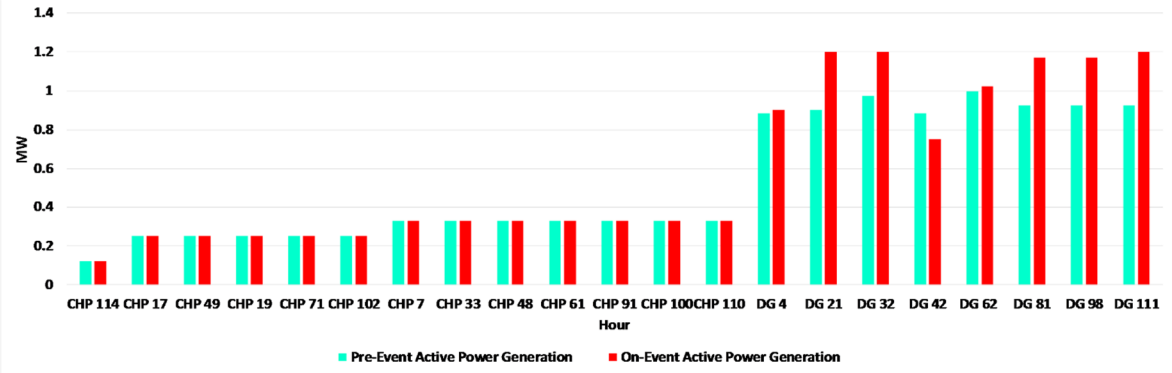

(a)

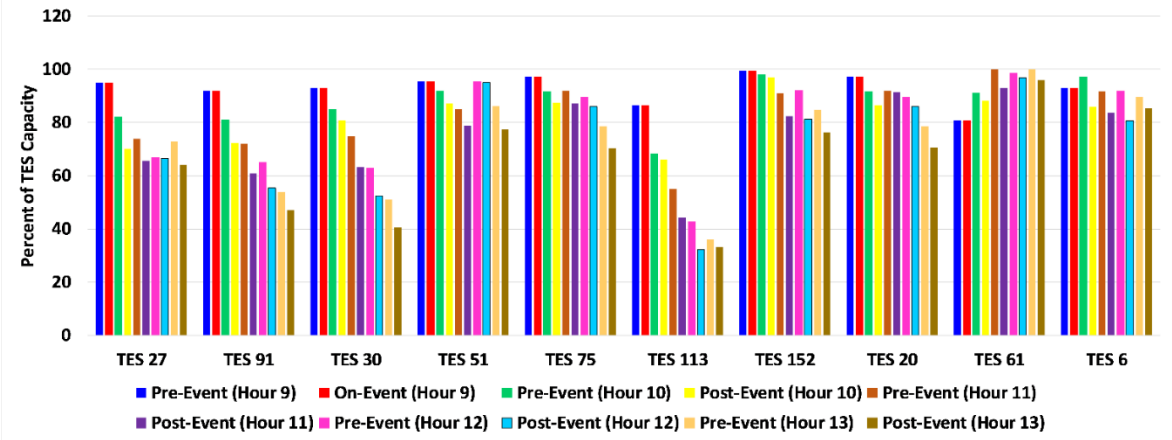

(b)

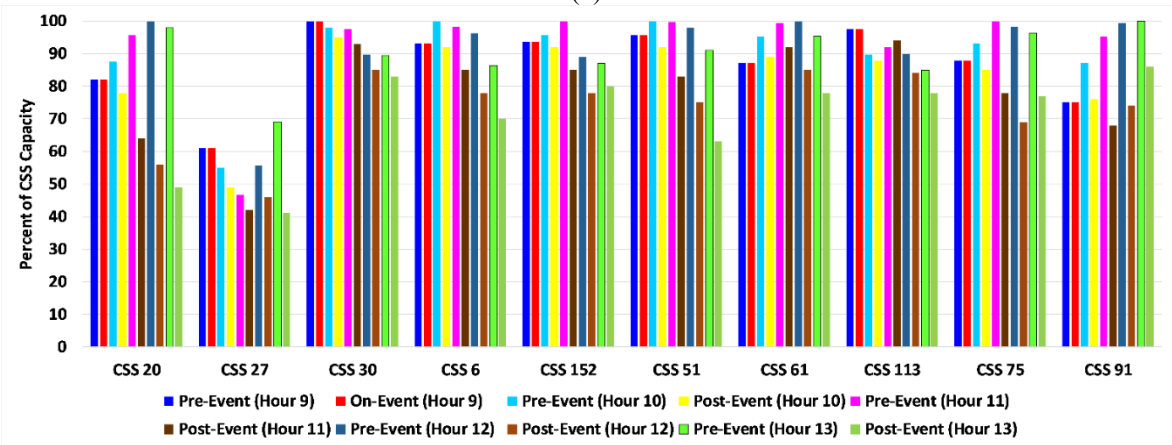

(c)

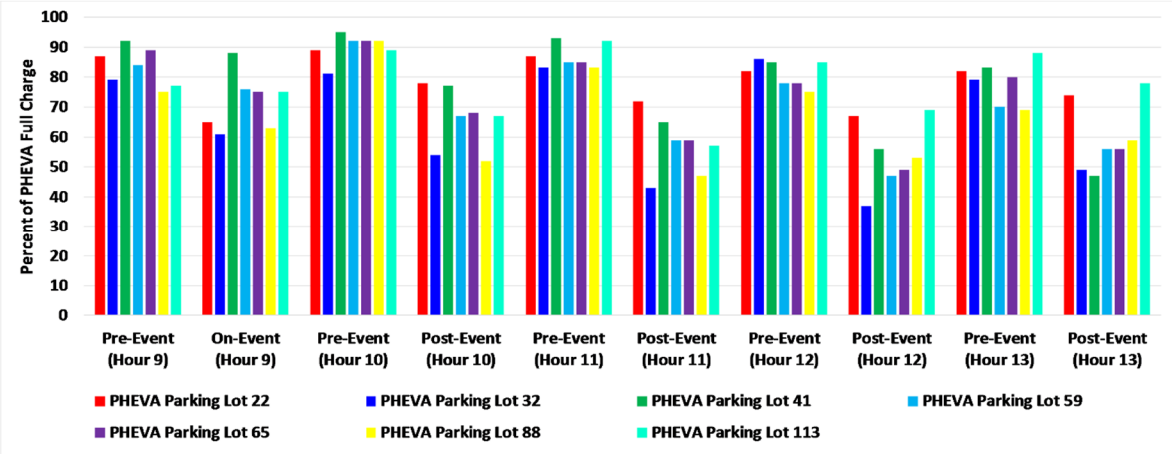

(d)

Fig. 19. (a) The estimated optimal pre-event and on-event dispatch values of CHPs, (b) The estimated optimal pre-event and on-event dispatch values of thermal energy storages, (c) The estimated optimal pre-event and on-event dispatch values of cool storage systems. (d) The estimated optimal pre-event and on-event dispatch values of PHEVAs.

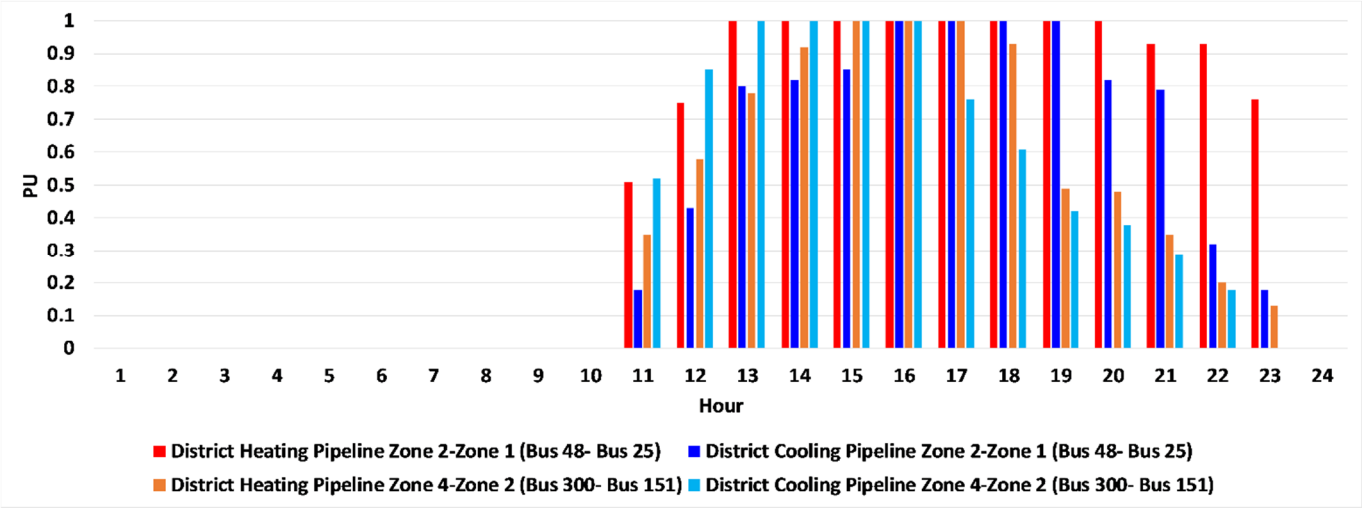

Fig. 20. The estimated pre-event and on-event dispatch of district heating and cooling pipelines of zone 2-zone 1 and zone 4 - zone 2.

The direct load control procedures were implemented for the heating and cooling loads. The maximum values of estimated heating load reduction were 0.9948 MW (zone 1 for hour 14), 1.3746 MW (zone 2 for hour 12) and 1.321 MW (zone 5 for hour 11), respectively. Further, the maximum values of estimated cooling load reduction were 1.009 MW (zone 1 for hour 17), 1.231 MW (zone 2 for hour 19) and 0.7798 MW (zone 5 for hour 11), respectively. The proposed preventive/corrective framework has successfully determined the optimal value of the control risk parameter, the optimal preventive and corrective scheduling of DERs, and the multi-carrier energy network topology after extreme shock impacts.

5. Conclusion

This paper addressed a framework for optimal resilient operation and preventive/corrective actions of a multi-carrier energy distribution system that utilized electrical, heating and cooling distributed energy resources. The model considered the plug-in hybrid electric vehicle aggregators and demand response aggregators in the preventive/corrective scheduling of the system. Further, the proposed three-stage algorithm utilized the pre-event robust optimization for a day-ahead horizon that adaptively determined the optimal parameter of risk control. Based on the pre-event scheduling of system resources, the real-time market optimization was carried out in the second stage. The post-event status of the system was investigated in the third stage and the effectiveness of corrective actions was explored and simulated. The optimal switching of electrical switches, on/off control of district heating and cooling control valves were modelled in the third stage problem. In the case study, the 123-bus test system was assessed and 600 external shocks were considered. The procedure reduced the expected cost of the system by about 74.59% for the worst-case external shock. Further, the algorithm reduced the aggregated expected value of the objective function of the third stage problem by about 57.73% for all of the 600 cases of the considered external shock scenarios. In conclusion, the proposed algorithm optimally dispatched the system resources for preventive/corrective actions and adaptively determined the optimal value of the risk control parameter.

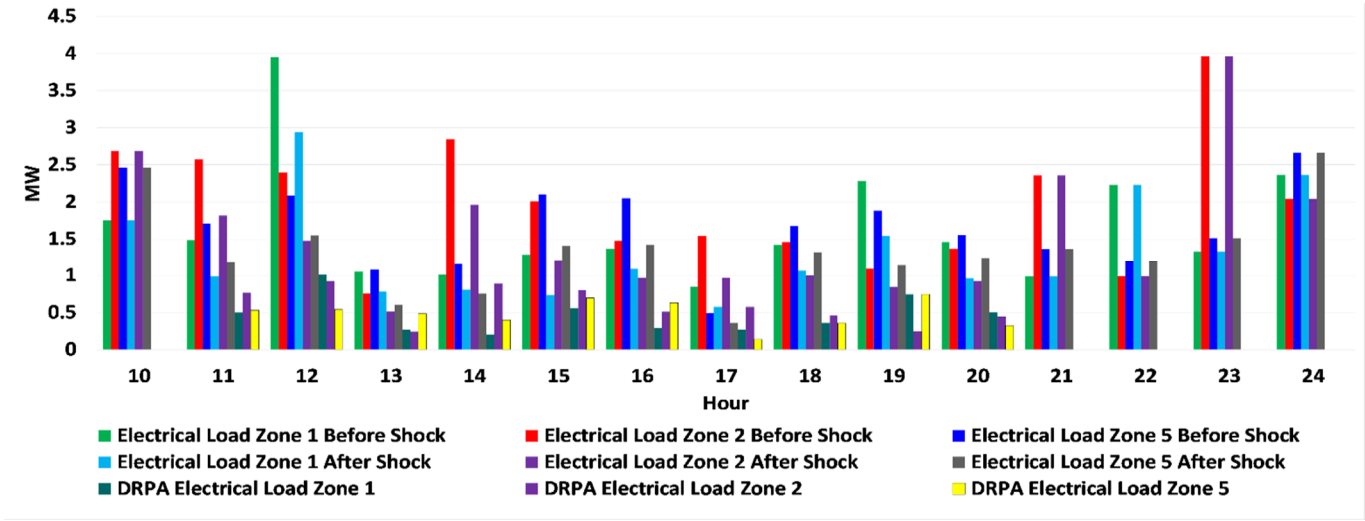

(a)

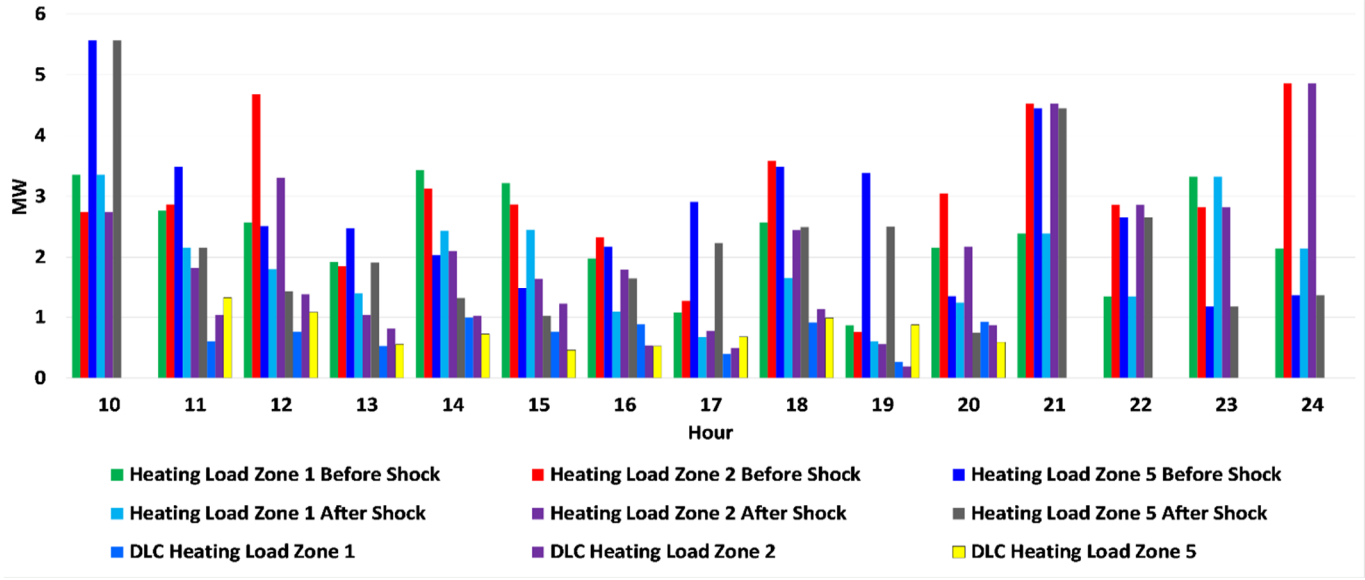

(b)

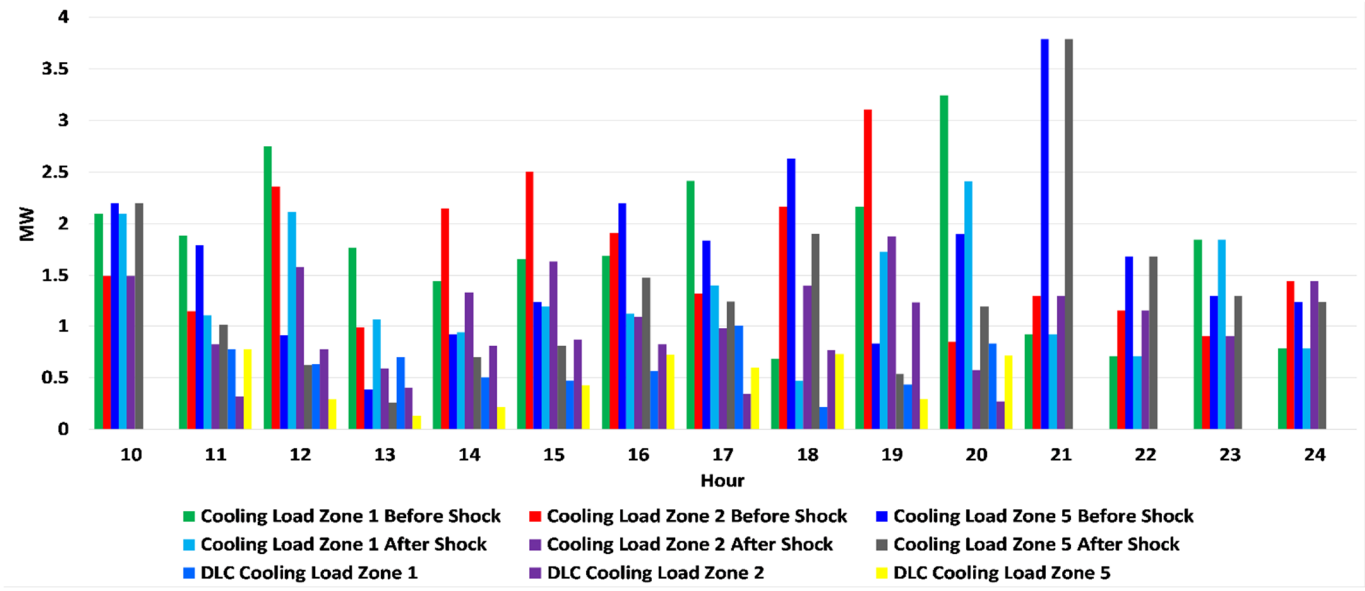

(c)

Fig. 21 (a), (b), (c). The estimated pre-event and on-event electrical load, heating load and cooling load of the external shock affected zones.

Acknowledgement

J.P.S. Catalão acknowledges the support by FEDER funds through COMPETE 2020 and by Portuguese funds through FCT, under POCI-01-0145-FEDER-029803 (02/SAICT/2017).

References

1- W. Kröger, E. Zio, "*Vulnerable Systems"*, 2011, Springer.

2- S. Chanda, A.K. Srivastava,"Defining and enabling resiliency of electric distribution systems with multiple microgrids", *IEEE Trans. on Smart Grid,* 2016, **7**, pp. 2859-2868.

3- M. Zadsar, M.R. Haghifam, S.M.M. Larimi, "Approach for self-healing resilient operation of active distribution network with microgrid", *IET Gener. Transm. Distrib*., 2017, **11**, pp. 4633-4643.

4- A. Hussain, V.H. Bui, H.M. Kim,"Microgrids as a resilience resource and strategies used by microgrids for enhancing resilience", *Applied Energy,* 2019, **240,** pp. 56-72.

5- B. Balasubramaniam, P. Saraf, R. Hadidi, E.B. Makram," Energy management system for enhanced resiliency of microgrids during islanded operation", *Electr. Power Syst. Res*., 2016, **137**, pp. 133-141.

6- S. Mousavizadeh, T.G. Bolandi, M.R. Haghifam, M. Moghimi, J. Lu,"Resiliency analysis of electric distribution networks: A new approach based on modularity concept", *Int. J. Electr. Power Energy Syst*., 2020, **117**, 105669.

7- A.R. Sayed, C. Wang, T. Bia, "Resilient operational strategies for power systems considering the interactions with natural gas systems", *Applied Energy,* 2019, **241,** pp. 548-566.

8- S. Manshadi, M.E. Khodayar, "Resilient operation of multiple energy carrier microgrids", *IEEE Trans. on Smart Grid,* 2015, **6**, pp. 2283-2292.

9- T. Khalili, M. Tarafdar Hagh, S. Gassem Zadeh, S. Maleki,"Optimal reliable and resilient construction of dynamic self-adequate multi-microgrids under large-scale events", *IET Gener. Transm. Distrib*., 2019, **10**, pp. 1750 - 1760.

10- A. Khodaei, "Resiliency oriented microgrid optimal scheduling", *IEEE Trans. on Smart Grid,* 2014, **5**, pp. 1584-1591.

11- Z. Wang, J. Wang, "Self-healing resilient distribution systems based on sectionalization into microgrids", *IEEE Trans. on Power Sys.,* 2015, **30**, pp. 3139-3149.

12- H. Afrakhte, P. Bayat, "A contingency based energy management strategy for multi-microgrids considering battery energy storage systems and electric vehicles", *J. Energy Storage*, 2020, **27**, 101087.

13- V. Hosseinnezhad, M. Rafiee, M. Ahmadian, P. Siano, "Optimal island partitioning of smart distribution systems to improve system restoration under emergency conditions", *Int. J. Electr. Power Energy Syst*., 2018, **97**, pp. 155-164.

14- J. Zhu, Y. Yuan, W. Wang," An exact microgrid formation model for load restoration in resilient distribution system", *Int. J. Electr. Power Energy Syst*., 2020, **116**, pp. 105568.

15- M. Figueroa-Candia, F.A. Felder, D.W. Coit, "Resiliency-based optimization of restoration policies for electric power distribution systems", *Electr. Power Syst. Res.*, 2018, **161**, pp. 188-198.

16- V. Davatgaran, M. Saniei, S. Saeidollah Mortazavi, "Smart distribution system management considering electrical and thermal demand response of energy hubs", *Energy*, 2019, **169**, pp. 38-49.

17- B. Zhang, Q. Lia, L. Wang, W. Feng," Robust optimization for energy transactions in multi-microgrids under uncertainty", *Applied Energy*, 2018, **217**, pp. 346–360.

18- F. Samadi Gazijahani, J. Salehi, "Integrated DR and reconfiguration scheduling for optimal operation of microgrids using Hong's point estimate method ", *Electr. Power Syst. Res.*, 2018, **99**, pp. 481-492.

19- A. Rabiee, M. Sadeghi, J. Aghaei, A. Heidari, "Optimal operation of microgrids through simultaneous scheduling of electrical vehicles and responsive loads considering wind and PV units uncertainties", *Renew. Sustain. Energy Rev.,* 2016, **57**, pp. 721-739.

20- M. Alipour, B. Mohammadi-Ivatloo, K. Zare, "Stochastic risk-constrained short-term scheduling of industrial cogeneration systems in the presence of demand response programs", *Applied Energy,* 2014, **136,** pp. 393-404.

21- S. Tabatabaee, S. S. Mortazavi, T. Niknam, "Stochastic scheduling of local distribution systems considering high penetration of plug-in electric vehicles and renewable energy sources", *Energy,* 2017, **121** , pp. 480-490.

22- J. Aghaei, V.G. Agelidis, M. Charwand, F. Raeisi, A. Ahmadi, A. Esmaeel Nezhad, A. Heidari, "Optimal Robust Unit Commitment of CHP Plants in Electricity Markets Using Information Gap Decision Theory", *IEEE Trans. on Smart Grid,* 2017, **8** , pp. 2296-304.

23- M.H. Shams, M. Shahabi, M.E. Khodayar, "Stochastic day-ahead scheduling of multiple energy carrier microgrids with demand response", *Energy,* 2018, **155** , pp. 326-338.

24- M.R. Sarker , H. Pandžić, K. Sun, M.A. Ortega-Vazquez, "Optimal operation of aggregated electric vehicle charging stations coupled with energy storage", *IET Gener. Transm. Distrib*., 2018, **12**, pp. 1127-1136.

25- Y. Liu, L. Guo, C. Wang, "A robust operation-based scheduling optimization for smart distribution networks with multi-microgrids", *Applied Energy*, 2018, **228**, pp. 130-140.

26- S. M. Bagher Sadati, J. Moshtagh, M.R. Shafie-khah, J.P.S. Catalão, "Smart distribution system operational scheduling considering electric vehicle parking lot and demand response programs", *Electr. Power Syst. Res.*, 2018, **160**, pp. 404-418.

27- Z. Wang , A. Negash, D.S. Kirschen, "Optimal scheduling of energy storage under forecast uncertainties", *IET Gener. Transm. Distrib*., 2017, **11**, pp. 4220-4226.

28- F. Varasteh, M. Setayesh Nazar, A. Heidari, M.R. Shafie-khah, J. P. S. Catalão, “Distributed energy resource and network expansion planning of a CCHP based active microgrid considering demand response programs”, *Energy*, 2019, **172**, pp. 19-105.

29- M.E. Khodayar, L.Wu, M Shahidehpour,” Hourly coordination of electric vehicle operation and volatile wind power generation in SCUC”, *IEEE Trans. on Smart Grid,* 2012, **3** , pp. 1271-1279.

30- J.V. Rhein, G.P. Henze, N. Long, Y. Fu, “Development of a topology analysis tool for fifth-generation district heating and cooling networks”, *Energy Convers. Manage.*, 2019, **196**, pp. 705-716.

31- Zeyu Wang , Ahlmahz Negash, Daniel S. Kirschen, “Optimal scheduling of energy storage under forecast uncertainties”, *IET Gener. Transm. Distrib*., 2017, **11**, pp. 4220-4226.

32- Y. Wang, C. Chen, J.Wang, R.Baldick,”Research on resilience of power systems under natural disasters—a review”, *IEEE Trans. on Power Sys.,* 2016, **31**, pp. 1604-1613.

33- M. Setayesh Nazar, A. Heidari,”Multi-stage resilient distribution system expansion planning considering non-utility gas-fired distributed generation, power system resilience”, in Tabatabaei, NM, et al, (eds): *Power systems resilience*, 2018, pp. 192-222, Springer.

34- J. F. Franco, M. J. Rider, M. Lavorato, and R. Romero, "Optimal conductor size selection and reconductoring in radial distribution systems using a mixed-integer LP approach," *IEEE Trans. on Power Sys.,* 2012, **28**, pp. 10-20.

35- M. Carrión and J. M. Arroyo, "A computationally efficient mixed-integer linear formulation for the thermal unit commitment problem," *IEEE Trans. on Power Sys.,* 2006, **21**, pp. 1371-1378.

36- A. Ben-Tal and A. Nemirovski, “On polyhedral approximations of the second-order cone", *Mathematics of Oper Res,* 2001, **26**, pp. 193-205.

37- X. Lin, Z.Tian, Y.Lu, H. Zhang, J. Niu,”Short-term forecast model of cooling load using load component disaggregation”, *Applied Thermal Energy*, 2019,113630.

38- H. Heitsch, W.Romisch,”Scenario reduction algorithms in stochastic programming”, *Comput. Optim. Application,* 2003, 24, pp. 187–206.

39- M. Setayesh Nazar, AE. Fard, A. Heidari, M.R. Shafie-khah, J.P.S. Catalão, ”Hybrid model using three-stage algorithm for simultaneous load and price forecasting”, *Electr. Power Syst. Res.*, 2018, **165**, pp. 214-228.

40- J.Zhang, B.M.Hodge, S.Lu, H.F. Hamann, B. Lehman , J.Simmons, E.Campos,V. Banunarayanan, J.Black, J.Tedesco, “Baseline and target values for regional and point PV power forecasts: Toward improved solar forecasting”, *Solar Energy,* 2015, **122**, pp. 804-819.

41- B.M. Hodge, A. Florita, J. Sharp, M. Margulis, D. Mcreavy, “The value of improved short term wind power forecasting”, *National Renewable Energy Laboratory (NREL) technical report*, 2015.